Ecological Applications, 24(7), 2014, pp. 1651–1669
© 2014 by the Ecological Society of America

Spectroscopic determination of leaf morphological and biochemical traits for northern temperate and boreal tree species

Shawn P. Serbin,[1,3] Aditya Singh,[1] Brenden E. McNeil,[2] Clayton C. Kingdon,[1] and Philip A. Townsend[1]

[1]*Department of Forest and Wildlife Ecology, University of Wisconsin, Madison, Wisconsin 53706 USA*
[2]*Department of Geology and Geography, West Virginia University, Morgantown, West Virginia 26506 USA*

Abstract. The morphological and biochemical properties of plant canopies are strong predictors of photosynthetic capacity and nutrient cycling. Remote sensing research at the leaf and canopy scales has demonstrated the ability to characterize the biochemical status of vegetation canopies using reflectance spectroscopy, including at the leaf level and canopy level from air- and spaceborne imaging spectrometers. We developed a set of accurate and precise spectroscopic calibrations for the determination of leaf chemistry (contents of nitrogen, carbon, and fiber constituents), morphology (leaf mass per area, M_{area}), and isotopic composition ($\delta^{15}N$) of temperate and boreal tree species using spectra of dried and ground leaf material. The data set consisted of leaves from both broadleaf and needle-leaf conifer species and displayed a wide range in values, determined with standard analytical approaches: 0.7–4.4% for nitrogen (N_{mass}), 42–54% for carbon (C_{mass}), 17–58% for fiber (acid-digestible fiber, ADF), 7–44% for lignin (acid-digestible lignin, ADL), 3–31% for cellulose, 17–265 g/m^2 for M_{area}, and −9.4‰ to 0.8‰ for $\delta^{15}N$. The calibrations were developed using a partial least-squares regression (PLSR) modeling approach combined with a novel uncertainty analysis. Our PLSR models yielded model calibration (independent validation shown in parentheses) R^2 and the root mean square error (RMSE) values, respectively, of 0.98 (0.97) and 0.10% (0.13%) for N_{mass}, $R^2 = 0.77$ (0.73) and RMSE = 0.88% (0.95%) for C_{mass}, $R^2 = 0.89$ (0.84) and RMSE = 2.8% (3.4%) for ADF, $R^2 = 0.77$ (0.69) and RMSE = 2.4% (3.9%) for ADL, $R^2 = 0.77$ (0.72) and RMSE = 1.4% (1.9%) for leaf cellulose, $R^2 = 0.62$ (0.60) and RMSE = 0.91‰ (1.5‰) for $\delta^{15}N$, and $R^2 = 0.88$ (0.87) with RMSE = 17.2 g/m^2 (22.8 g/m^2) for M_{area}. This study demonstrates the potential for rapid and accurate estimation of key foliar traits of forest canopies that are important for ecological research and modeling activities, with a single calibration equation valid over a wide range of northern temperate and boreal species and leaf physiognomies. The results provide the basis to characterize important variability between and within species, and across ecological gradients using a rapid, cost-effective, easily replicated method.

Key words: foliar chemistry; forests; partial least-squares regression, PLSR; plant functional traits; reflectance spectroscopy; remote sensing.

Introduction

The nutritional and morphological properties of leaves within plant canopies are strong predictors of photosynthetic capacity and biogeochemical cycling in ecosystems (Aber and Melillo 1982, Green et al. 2003, Wright et al. 2004, Shipley et al. 2005, Santiago 2007, Cornwell et al. 2008). Variations in foliar morphology, quantified as the leaf dry mass per leaf area (M_{area}; g/m^2) or the reciprocal (specific leaf area, SLA), correspond to the fundamental tradeoff in leaf construction costs vs. light-intercepting surface area and are driven by a range of environmental controls (Niinemets 2007, Poorter et al. 2009). Foliar nitrogen, on a mass (N_{mass}; %) or area (N_{area}; g/m^2) basis, is strongly related to the photosynthetic capacity of leaves, because it is a fundamental component of light-harvesting pigments and photosynthetic machinery, including the enzyme RuBisCo (Field and Mooney 1986, Evans 1989). In particular, nitrogen represents a primary limiting nutrient in temperate and boreal tree species (LeBauer and Treseder 2008).

Other chemical compounds such as lignin and cellulose are invested in leaf structural components and, along with leaf carbon concentration (C_{mass}; %), determine the recalcitrant characteristics of canopy foliage (Aber and Melillo 1982, Santiago 2007, Fortunel et al. 2009), thereby influencing the nutrient cycling potential of ecosystems. There has also been an increasing interest in the use of stable isotopes as a source of important information on the relationships between plants and their environment (e.g., Hobbie and Hobbie 2006, Compton et al. 2007, Bowling et al. 2008,

Manuscript received 12 November 2013; revised 21 February 2014; accepted 7 March 2014; final version received 1 April 2014. Corresponding Editor: W. J. D. van Leeuwen.

[3] Present address: Biological, Environmental and Climate Sciences Department, Brookhaven National Laboratory, Upton, New York 11973 USA. E-mail: serbin@wisc.edu

/JTITAN/Production/e/ecap/live_jobs/ecap-24-07/ecap-24-07-08/layouts/ecap-24-07-08.3d ■ Monday, 22 September 2014 ■ 1:42 pm ■ Allen Press, Inc. ■ Page 1651 MS 13-2110

Helliker and Richter 2008, Craine et al. 2009). In the case of nitrogen, $\delta^{15}N$ provides an integrated assessment of the nitrogen cycling properties of a stand (Robinson 2001, Compton et al. 2007) and especially the associated microbial communities that preferentially assimilate different isotopes at different rates (Hobbie and Hobbie 2006, Craine et al. 2009). Thus, the ability to characterize variation in key leaf functional traits among species and across ecosystems is central to improving our understanding of nutrient cycling and carbon assimilation by plants.

In the last few decades, remote sensing has played an increasingly important role in the study of plant chemistry (e.g., Curran 1989, Asner and Martin 2009, Kokaly et al. 2009, Ustin et al. 2009). Reflectance spectroscopy of fresh leaves or dried and ground leaf material has shown the potential to link leaf optical properties with a range of foliar traits, including pigments, water content, nitrogen, dry matter, cellulose, and lignin (e.g., Card et al. 1988, McLellan et al. 1991*a*, *b*, Bolster et al. 1996, Richardson and Reeves 2005, Petisco et al. 2006). These studies led to the development of a number of leaf-level radiative transfer models, including PROSPECT (Jacquemoud and Baret 1990, Feret et al. 2008), Liberty (Dawson et al. 1998), and LEAFMOD (Ganapol et al. 1998), which provide a mechanistic understanding of the coordination between leaf properties and spectral reflectance. At the canopy scale, early research into the use of imaging spectrometers (Peterson et al. 1988, Wessman et al. 1988*b*, Matson et al. 1994) illustrated the potential for quantifying select canopy chemical properties, including nitrogen and lignin, but with some sensor and statistical limitations (Grossman et al. 1996). Later studies determined that a range of foliar traits could be remotely sensed through the use of improved imaging spectrometers (Curran et al. 1997, Martin and Aber 1997, Smith et al. 2003, Townsend et al. 2003), providing a means to study ecosystem functioning in a spatial context (Ollinger et al. 2002, Smith et al. 2002, Ollinger and Smith 2005, McNeil et al. 2008, Deel et al. 2012, Dahlin et al. 2013). Recently, it has been demonstrated that spectroscopy can simultaneously provide estimates of a range of foliar nutrients and morphology at the leaf and canopy scales within diverse tropical ecosystems (e.g., Asner and Martin 2008, Asner et al. 2011*a*, Doughty et al. 2011).

Refinement of generalized algorithms measuring foliar traits from reflectance spectroscopy of dried and ground leaf material can not only aid further development of generalized algorithms capable of using imaging spectrometer data to make canopy-level trait measurements, but it can also catalyze spatially extensive ecological research by providing a rapid and inexpensive means for measuring trait variation across multiple canopy heights, diverse species, and distinct geographic settings. In this study, we examine the ability to make generalized estimates of a suite of key leaf biochemical, nutritional, and morphological properties, namely leaf C_{mass}, N_{mass}, the relative abundance of stable nitrogen isotopes ($\delta^{15}N$), M_{area} (LMA), lignin, cellulose, and fiber (lignin and cellulose), using leaf-level reflectance spectroscopy of dried and ground (i.e., homogenized) leaf material. Our primary goal is to demonstrate a generalized approach for estimating each leaf property, along with its variation, among species and functional groups, as it relates to within-canopy radiation levels. Specifically, we (1) evaluate the capacity to accurately estimate seven leaf traits using reflectance spectroscopy at the leaf level; (2) identify regions of the spectrum important to retrieval of these traits; and (3) test the extent to which we can generalize the predictions of leaf traits across species and geographic locations.

Materials and Methods

Study sites

We sampled a broad range of canopy dominant tree species in natural forests of the north central and northeastern United States (Fig. 1a, Table 1) during the 2008–2011 growing seasons (i.e., June–September). The data set comprises the most common tree species found within the forests of this region (Appendix A), and the sample locations span a large range in climatic conditions (Fig. 1, Table 1). The forests in this region are of high environmental, societal, and economic importance (White et al. 2005) and have been the focus of many important ecological and global change research projects over the last few decades (e.g., Curtis 1959, Pastor et al. 1984, Frelich and Reich 1995, Mitchell et al. 1996, Fassnacht and Gower 1999, Schulte et al. 2005, Wolter et al. 2008, Burton et al. 2011, Couture et al. 2011). The study region includes the Chequamegon Ecosystem Atmosphere Study (ChEAS), the goal of which is to characterize the environmental controls and disturbance impacts on forest carbon and water fluxes within northern temperate forests (e.g., Burrows et al. 2003, Ahl et al. 2004, Cook et al. 2008, Desai et al. 2008, Ewers et al. 2008). In addition, the Blackhawk Island, Wisconsin, USA study site is the location of several pioneering studies illustrating the potential for imaging spectroscopy to successfully map ecosystem properties related to carbon and nutrient cycling (e.g., Wessman et al. 1988*b*, Martin and Aber 1997). Finally, two of our sites contained old-growth hemlock (*Tsuga canadensis*), both hardwood forests comprising the few remnant forests in the region that did not experience major logging during the last century (Frelich and Lorimer 1991).

Field methods

Samples were collected from 165 plots across the study region. At each plot, individual canopies were sampled using a shotgun or line launcher (Cascade Rescue, Sandpoint, Idaho, USA) outfitted with a rope saw to retrieve sunlit foliage from the upper canopy (top one-third) and mid-canopy partially shaded leaves

/TITAN/Production/e/ecap/live_jobs/ecap-24-07/ecap-24-07-08/layouts/ecap-24-07-08.3d ■ Monday, 22 September 2014 ■ 1:42 pm ■ Allen Press, Inc. ■ Page 1652 MS 13-2110

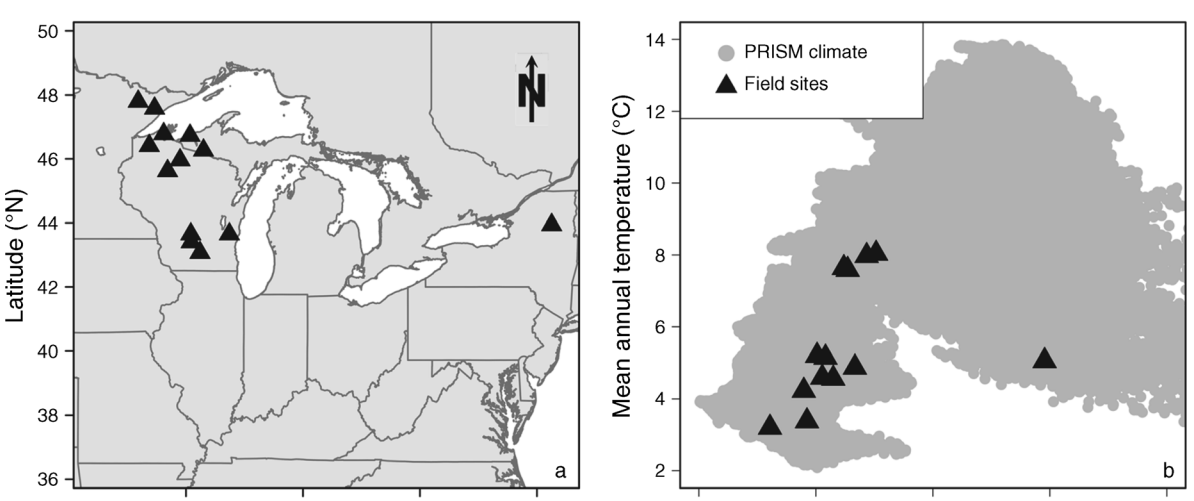

FIG. 1. The location of the field study sites (Table 1) presented in (a) geographic and (b) climate space. Gray area in panel (b) indicates the range of climatic space in the eastern United States. Our field sites cover a considerable portion of the range in climatic conditions in temperate and sub-boreal regions of the conterminous United States, as indicated by the climatic envelope in panel (b).

(middle one-third). Bottom canopy (bottom one-third), fully shaded leaves were sampled with a pole pruner or hand shears. In contrast to studies focused exclusively on remote sensing (e.g., Asner et al. 2011*a*), we collected both sunlit and shaded foliage to examine the generality of the methods across broad species and functional groups, but also the ability of the methods to capture the strong modifications in leaf traits that occur with variation in light intensity within a canopy (Niinemets 2007, Poorter et al. 2009, Ollinger 2011).

The samples were immediately sealed in large polyethelyne bags containing moist paper towels to maintain moisture (Foley et al. 2006) and placed into coolers for transport within 1–3 hours to a field laboratory for further processing. Immediately, the foliar fresh mass (g) and leaf area (cm^2) for samples intended for chemical analysis and/or spectral collection were determined using a precision balance and cork-borers for broadleaf species or a flatbed scanner for needleleaf samples. The fresh leaf area for needleleaf species was then determined using the scanned images of the weighed needles and analyzed with the open-source ImageJ software (Abràmoff et al. 2004) using particle recognition routines described by Richardson et al. (2001). In addition, we separated needleleaf species into age classes. For pines, we separated needles into new (current year foliage) and

TABLE 1. Summary of field data collection sites located in the upper Midwest and northeastern United States.

Site	No. plots	Elevation range (m)	MAP (mm)	MAT (°C)
Michigan				
Ottawa National Forest	5	460–541	805	4.3
Porcupine Mountains	5	272–391	867	4.8
Minnesota				
Finland State Forest/North Shore	9	384–591	785	3.4
Superior National Forest	5	437–459	722	3.2
New York				
Adirondack Park	42	365–770	1191	5.1
Wisconsin				
Baraboo Hills	12	318–423	887	7.9
Bayfield	4	295–367	830	4.6
Blackhawk Island	10	262–264	854	7.6
Chequamegon National Forest	19	470–520	811	4.6
Flambeau State Forest	4	425–435	817	5.2
Kettle Moraine	5	312–380	848	7.6
Madison	31	260–300	903	8.0
Pine Barrens	14	275–381	802	5.2

Notes: Range in elevation derived from the GTOPO30 data set. Mean annual precipitation (MAP) and mean annual temperature (MAT) data are from PRISM (Daly et al. 1994).

/TITAN/Production/e/ecap/live_jobs/ecap-24-07/ecap-24-07-08/layouts/ecap-24-07-08.3d ■ Monday, 22 September 2014 ■ 1:42 pm ■ Allen Press, Inc. ■ Page 1653 MS 13-2110

old (previous years foliage), while for spruce, fir, and hemlock trees, we maintained three separate classes of new, previous year, and older foliage. In the lab, the same leaf discs and needle samples, separated by age and position within the canopy, were oven dried at 70°C for 72 h to obtain oven-dry mass (g). These data, combined with the area measurements, were then used to calculate the specific leaf area (SLA; m^2/kg) and leaf mass per area (1/SLA, M_{area}; g/m^2).

Tissue chemistry

Oven-dried samples were ground and homogenized using a blade grinder and stored in a desiccator. Samples were again oven dried the night before sample preparation and allowed to cool for 1 h prior to preparation to ensure proper measurement of material dry mass. We determined foliar nitrogen concentration (N_{mass}; %) via Dumas combustion using the Vario Macro CHN (Elementar, Hanau, Germany). Results are reported on a dry-mass ash-included basis.

Leaf ^{15}N:^{14}N ratio was determined on a subset of samples via isotope ratio mass spectrometry (IRMS) at the UC Davis Stable Isotope Facility (SIF; Davis, California, USA). Results were expressed in standard δ notation where foliar ^{15}N:^{14}N ratios are reported relative to the atmospheric N_2 ratio as $\delta^{15}N$ (‰) = $(R_{sample}/R_{atmo} - 1) \times 1000$, where $R_{atmo} = 0.0036765$. The $\delta^{15}N$ of atmospheric N_2 is by definition 0.0‰. The concentrations of leaf fiber (acid detergent fiber, determined as cellulose + lignin) and lignin were determined gravimetrically using sequential extraction in a hot acid-detergent solution in an Ankom 200 Fiber Analyzer (Ankom Technology, Macedon, New York, USA) and incubation in 72% H_2SO_4. Cellulose was calculated as the difference between fiber and lignin. While this method may not be precise for isolating fiber/lignin (Brinkmann et al. 2002), it was deemed sufficient for examining relative variation in recalcitrance properties among species and sites.

Spectroscopy of the dried and ground leaf material

We collected leaf reflectance spectra on dried, ground, and homogenized leaf material using an ASD FieldSpec 3 full-range spectroradiometer (Analytical Spectral Devices, Boulder, Colorado, USA) configured for fast and consistent collection of spectra. We designed and built a "probe press" apparatus; a Dremel Workstation (Dremel, Racine, Wisconsin, USA) drill press modified for use with an ASD plant-probe fore optic, a fitted aluminum sample cup painted matte black with Krylon Ultra-Flat Black (Krylon Industrial, Cleveland, Ohio, USA), and an integrated Effetto Mariposa, Giustaforza Professional precision torque wrench handle (Effetto Mariposa, Bra, Italy), which was used to collect spectra on the dried leaf material. The plant probe contains a light source which is perpendicular to the contact surface, and the end of a bare fiber-optic cable bundle mounted at 42° to perpendicular; this configuration minimizes specular reflectance.

Through trial-and-error, it was determined that 800 mg of leaf material provided the most consistent and stable results between sample replicates (<0.1% variation, data not shown). The loosely packed dry leaf material was weighed and poured into the sample cup, leveled, then the probe was depressed into the sample material with 2 N·m of torque. On a single sample, we collected three spectra, loosened and mixed the sample in the cup, and then collected another three spectra. Between each of the six scans, we turned the sample cup to minimize systematic bias that could arise from orientation of the material and/or due to probe characteristics. All spectral observations underwent automated quality assurance/quality control, as well as a splice correction to ensure continuous spectra across detectors in the spectrometer before averaging in R, using package FieldSpectra to produce a single spectrum per sample (package *available online*).[4]

Leaf chemometric analysis

We utilized a partial least-squares regression (PLSR) modeling approach (Wold 1984, 2001, Geladi and Kowalski 1986, Serbin et al. 2012) using the PLS package (Mevik and Wehrens 2007) in the R open-source statistical environment (R Development Core Team 2013) to predict the target leaf traits from ASD spectra. PLSR is a standard statistical approach utilized in chemometric analyses and is superior to stepwise regression because it is designed to handle high predictor collinearity and/or situations where the number of predictor variables is equal to or higher than the number of observations. These situations lead to erroneous results with standard stepwise linear regression (Grossman et al. 1996). PLSR reduces the large predictor matrix (i.e., spectral reflectance data) down to a relatively few, noncorrelated latent components.

We split our data (Table 2 lists the number of observations for each trait) for model calibration (80%) and independent validation (20%), ensuring that both sets spanned the range of measured values for each trait. The calibration data were further split 70% to 30% via 1000 permutations to conduct uncertainty analysis (see *Materials and methods, evaluation of PLSR model performance and uncertainty analysis*), meaning that for any one of the 1000 permutations, a random 56% of the data were used for model development and 24% for model assessment and uncertainty analysis, while an unchanging 20% of the data were withheld entirely until the end of the process to evaluate the final models. We used a set percentage for validation for all traits to ensure consistency in the application of our analyses, with 20% specifically selected to ensure that trait with the lowest number of samples ($\delta^{15}N$, $n = 178$) had

[4] https://github.com/serbinsh/R-FieldSpectra

/TITAN/Production/e/ecap/live_jobs/ecap-24-07/ecap-24-07-08/layouts/ecap-24-07-08.3d ■ Monday, 22 September 2014 ■ 1:42 pm ■ Allen Press, Inc. ■ Page 1654 MS 13-2110

TABLE 2. Summary statistics for the measured leaf nutritional and morphological traits examined in this study.

Leaf property	No. samples	Broadleaf		Conifer		Global range
		Median	Range	Median	Range	
Leaf mass per area, M_{area} (g/m^2)	759	50.8	17.4–117.8	164.9	35.2–270.0	14.5–1515.6
Nitrogen content, N_{mass} (%)	544	2.92	1.3–4.4	1.4	0.7–2.33	0.3–6.4
Carbon content, C_{mass} (%)	540	48.6	44.1–52.4	50.6	46.8–53.6	40.5–54.1
δ^{15}N (‰)	178	−3.1	−6.6–0.8	−4.7	−9.4 to −0.5	−11.0–18.5
Fiber, ADF (%)	224	33.9	22.4–55.5	43.3	17.5–57.9	22.0–60.0
Lignin, ADL (%)	220	18.5	8.6–39.3	24.6	8.7–35.1	2.0–65.0
Cellulose (%)	205	15.7	9.7–27.8	17.9	8.8–27.7	5.0–44.0

Notes: This data was used in the calibration and validation data sets for the development of the partial least-squares regression (PLSR) models. ADF and ADL refer to acid-digestible fiber and lignin, respectively. Global range data for M_{area} and N_{mass} are derived from Wright et al. (2004) GLOPNET database, global range data for C_{mass} are derived from Kattge et al. (2011), global range data for δ^{15}N come from Craine et al. (2009), and global range for fiber, lignin, and cellulose come from various sources, in addition to this study (Bolster et al. 1996, Curran et al. 1997, Asner et al. 2011).

enough samples for calibration and uncertainty analysis. To avoid the potential to over-fit the calibration models, we optimized the number of PLSR components by minimizing the prediction residual sum of squares (PRESS) statistic (Chen et al. 2004). We calculated the PRESS statistic of successive model components through a cross-validation analysis. For the larger data sets (N_{mass}, C_{mass}, and M_{area}) we used a 10-fold cross-validation, while for the other variables (acid-digestible fiber [ADF], acid-digestible lignin [ADL], cellulose, δ^{15}N), we used leave-one-out cross-validation. Finally, the optimal number of components for each model was determined where the root mean square error (RMSE) of the PRESS statistics achieved a minimum (Wold et al. 2001), and successive PLSR components did not improve RMSE as assessed using a t test. Lastly, we calculated the variable importance of projections metric (VIP; Wold et al. 1994) on the final models to identify the regions of the spectrum that were significant to the prediction of the seven leaf traits.

We reviewed past studies (e.g., Curran 1989, Elvidge 1990, Fourty et al. 1996, Richardson and Reeves 2005, Petisco et al. 2006, Kleinebecker et al. 2009, Asner et al. 2011*a*, *b*), to select regions of the spectrum as a basis for predicting each foliar trait. For M_{area}, we incorporated the visible (VIS, 500–700 nm), near-infrared (NIR, 700–1300 nm), and shortwave-infrared (SWIR, 1300–2400 nm) spectrum, given the coordination of leaf structure with pigment and water absorption features that co-vary with M_{area} (Baret and Fourty 1997, Niinemets 2007). For ADF, ADL, cellulose, and δ^{15}N, we used a portion of the shortwave-infrared spectrum (SWIR, 1200–2400 nm) with well-documented lignocellulose and nitrogen absorption characteristics (Curran 1989). The N_{mass} and C_{mass} models used a slightly smaller range of wavelengths (1500–2400 nm) corresponding to the dominant structural and nitrogen absorption features (Curran 1989, Elvidge 1990). The body of literature indicates that the SWIR contains the salient spectral info for most traits (Curran 1989, Elvidge 1990, Kokaly et al. 2009), with the NIR being useful for M_{area} (Asner et al. 2011*b*) and δ^{15}N (Wang et al. 2007). Moreover, we used pseudo-absorption ($A = \log[1/R]$) for ADF, ADL, cellulose, and δ^{15}N rather than reflectance (R) based on results of previous studies (Table 4).

Evaluation of PLSR model performance and uncertainty analysis

We quantified the performance of each PLSR model using three main metrics: the coefficient of determination (R^2), the root mean square error (RMSE), and the model bias. We provide the RMSE value for each leaf trait in the units of measure as well as a percentage of

TABLE 3. Results of the PLSR modeling and cross-validation for each leaf trait.

Leaf property	Spectrum range (nm)	Treatment	No. components	R^2		RMSE		%RMSE	
				Cal.	Val.	Cal.	Val.	Cal.	Val.
M_{area}, (g/m^2)	500–2400	raw	11	0.91	0.87	17.2	22.8	7.4	10.1
N_{mass} (%)	1500–2400	raw	9	0.98	0.97	0.10	0.13	2.7	4.0
C_{mass} (%)	1200–2400	raw	12	0.77	0.73	0.88	0.95	9.2	11.1
δ^{15}N (‰)	1200–2400	log(1/R)	14	0.62	0.60	0.91	1.51	10.2	16.2
ADF (%)	1200–2400	log(1/R)	13	0.84	0.85	2.8	3.4	7.3	9.3
ADL (%)	1200–2400	log(1/R)	13	0.77	0.69	2.4	3.9	9.2	12.7
Cellulose (%)	1200–2400	log(1/R)	10	0.77	0.72	1.4	1.9	7.5	11.4

Note: Root mean square error (RMSE) percentage shows the error of each model as a percentage of the observed data range in the calibration (Cal.) and validation (Val.) data set, respectively. We used pseudo-absorption ($A = \log[1/R]$) for ADF, ADL, cellulose, and δ^{15}N rather than reflectance (R) based on results of previous studies.

/TITAN/Production/e/ecap/live_jobs/ecap-24-07/ecap-24-07-08/layouts/ecap-24-07-08.3d ■ Monday, 22 September 2014 ■ 1:42 pm ■ Allen Press, Inc. ■ Page 1655 MS 13-2110

TABLE 4. Comparison of PLSR model results among studies for the seven leaf functional traits.

Trait vegetation type	N	Spectra	Spectral region (m)	Spectral treatment	R^2 Cal.	R^2 Val.
N_{mass} (%)						
Temperate/boreal	544	dry	1500–2400	raw	0.98	0.98
Temperate/boreal	372	dry	400–2498	1D[log(1/R)]	0.97	0.97, 0.93, 0.86
Temperate/boreal	372	dry	400–2498	2D[log(1/R)]	0.98	0.97, 0.93, 0.88
Temperate/boreal	372	dry	400–2498	2D[log(1/R)]	0.97	0.97, 0.93, 0.84
Aleppo pine	84	dry	1100–2500	2D[log(1/R)]	0.94	
Holm oak	92	fresh	400–1100	log(1/R)	0.51	
Holm oak	92	fresh	1100–2500	log(1/R)	0.70	
Holm oak	92	fresh	400–2500	log(1/R)	0.56	
Holm oak	92	fresh	1100–2500	2D[log(1/R)]	0.89	
Holm oak	92	fresh	400–2500	2D[log(1/R)]	0.93	
Montane conifer	132	dry	400–1098	2D[log(1/R)]	0.95	0.84
Montane conifer	132	dry	1100–2498	2D[log(1/R)]	0.96	0.92
Mediterranean	182	dry	1100–2500	log(1/R)	0.96	0.94
Mediterranean	182	dry	1100–2500	1D[log(1/R)]	0.99	0.92
Mediterranean	182	dry	1100–2500	2D[log(1/R)]	0.99	0.94
Tropical forests	162	fresh	400–2500	raw	0.85	
Bog species	72	dry	1250–2350	log(1/R)	0.96	0.86
Bog species	72	dry	1250–2350	1D[log(1/R)]	0.99	0.93
Bog species	72	dry	1250–2350	2D[log(1/R)]	0.99	0.89
Humid tropical	6136	fresh	400–1050	raw	0.59	
Humid tropical	6136	fresh	400–2500	raw	0.77	
Tropical forests	159	fresh	400–2500	raw	0.83	
Wheat	359	fresh	400–2500	1D	0.92	
Wheat	253	dry	400–2500	1D	0.93	
C_{mass} (%)						
Temperate/boreal	540	dry	1200–2400	raw	0.77	0.73
Aleppo pine	84	dry	1100–2500	2D	0.99	
Montane conifer	72	dry	400–1098	log(1/R)	0.37	
Montane conifer	72	dry	1100–2498	2D[log(1/R)]	0.26	
Bog species	72	dry	1250–2350	log(1/R)	0.92	0.93
Bog species	72	dry	1250–2350	1D[log(1/R)]	0.94	0.93
Bog species	72	dry	1250–2350	2D[log(1/R)]	0.96	0.94
Humid tropical	6136	fresh	400–1050	raw	0.43	
Humid tropical	6136	fresh	400–2500	raw	0.71	
M_{area} (g/m^2)						
Temperate/ boreal	759	dry	500–2400	raw	0.91	0.87
Holm oak	373	fresh	400–1100	log(1/R)	0.88	
Holm oak	373	fresh	1100–2500	log(1/R)	0.96	
Holm oak	373	fresh	400–2500	log(1/R)	0.95	
Holm oak	373	fresh	400–1100	2D[log(1/R)]	0.95	
Holm oak	373	fresh	1100–2500	2D[log(1/R)]	0.97	
Holm oak	373	fresh	400–2500	2D[log(1/R)]	0.98	
Humid tropical	6136	fresh	400–1050	raw	0.82	
Humid tropical	6136	fresh	400–2500	raw	0.77	
Tropical forests	2871	fresh	400–2500	raw	0.85	
Tropical forests	159	fresh	400–2500	raw	0.90	
Wheat	179	fresh	400–2500	1D	0.90	
ADF (%)						
Temperate/Boreal	224	dry	1200–2400	log(1/R)	0.84	0.85
Montane conifer	132	dry	400–1098	2D[log(1/R)]	0.88	0.68
Montane conifer	132	dry	1100–2498	2D[log(1/R)]	0.96	0.89
Mediterranean	182	dry	1100–2500	log(1/R)	0.97	0.96
Mediterranean	182	dry	1100–2500	1D[log(1/R)]	0.98	0.96
Mediterranean	182	dry	1100–2500	2D[log(1/R)]	0.97	0.92
ADL (%)						
Temperate/boreal	220	dry	1200–2400	log(1/R)	0.77	0.69
Temperate/boreal	372	dry	400–2498	1D[log(1/R)]	0.88	0.88, 0.78, 0.73
Temperate/boreal	372	dry	400–2498	2D[log(1/R)]	0.88	0.89, 0.75, 0.69

/TITAN/Production/e/ecap/live_jobs/ecap-24-07/ecap-24-07-08/layouts/ecap-24-07-08.3d ■ Monday, 22 September 2014 ■ 1:42 pm ■ Allen Press, Inc. ■ Page 1656 MS 13-2110

TABLE 4. Extended.

Error measurement		
Cal.	Val.	Source
0.10†	0.13†	present study
0.11‡	0.11, 0.14, 0.25§	Bolster et al. (1996)¶
0.11‡	0.11, 0.14, 0.26§	Bolster et al. (1996)¶
0.11‡	0.11, 0.14, 0.27§	Bolster et al. (1996)¶
0.53‡		Gillon et al. (1999)#
1.8§		Ourcival et al. (1999)
1.3§		Ourcival et al. (1999)
1.9§		Ourcival et al. (1999)
1.0§		Ourcival et al. (1999)
1.0§		Ourcival et al. (1999)
0.06‡	0.12†	Richardson and Reeves (2005)
0.05‡	0.12†	Richardson and Reeves (2005)
1.18‡	0.79§	Petisco et al. (2006)
0.79‡	0.89§	Petisco et al. (2006)
0.93‡	0.76§	Petisco et al. (2006)
0.32†		Asner and Martin (2008)
0.09‡	0.10§	Kleinebecker et al. (2009)
0.08‡	0.08§	Kleinebecker et al. (2009)
0.14‡	0.09§	Kleinebecker et al. (2009)
0.50†		Asner et al. (2011*a*)
0.39†		Asner et al. (2011*a*)
0.45†		Doughty et al. (2011)
0.37‡		Ecarnot et al. (2013)
0.27‡		Ecarnot et al. (2013)
0.88†	0.95†	this study
0.28‡		Gillon et al. (1999)#
0.89‡		Richardson and Reeves (2005)
0.96‡		Richardson and Reeves (2005)
0.97‡	0.93§	Kleinebecker et al. (2009)
0.91‡	0.87§	Kleinebecker et al. (2009)
0.81‡	0.86§	Kleinebecker et al. (2009)
2.42†		Asner et al. (2011*a*)
1.90†		Asner et al. (2011*a*)
17.2†	22.8†	this study
15.35§		Ourcival et al. (1999)
10.69§		Ourcival et al. (1999)
10.65§		Ourcival et al. (1999)
10.53§		Ourcival et al. (1999)
7.87§		Ourcival et al. (1999)
8.34§		Ourcival et al. (1999)
0.50		Asner et al. (2011*a*)
0.39		Asner et al. (2011*a*)
15.40		Asner et al. (2011*b*)
18.7†		Doughty et al. (2011)
6.3‡		Ecarnot et al. (2013)
2.8†	3.4†	this study
1.74‡	3.72†	Richardson and Reeves (2005)
1.03‡	2.23†	Richardson and Reeves (2005)
1.82‡	1.42§	Petisco et al. (2006)
1.64‡	1.47§	Petisco et al. (2006)
2.09‡	1.90§	Petisco et al. (2006)
2.4†	3.9†	this study
1.61‡	1.60, 1.69, 5.16§	Bolster et al. (1996)¶
1.62‡	1.53, 1.74, 5.67§	Bolster et al. (1996)¶

the sample data range (i.e., %RMSE) following Feilhauer et al. (2010) and Asner et al. (2011*a*).

As noted, we utilized a 1000× permutation test of each PLSR model to characterize the model calibration performance based on an iterative 70% to 30% split of the calibration data drawn from across the data range for each leaf trait. From this, we generated new estimates for the iteratively removed samples based on the retained samples and the previously determined optimal number of PLSR components. This was done to test stability and the generality of the models using different sets of calibration data (Serbin et al. 2012), and to estimate error distributions for each target leaf trait based on the uncertainty in trait measurements, spectral data, and statistical approach. We averaged model coefficients across the 1000 permutations to generate a mean PLSR model as well as means and distributions of all of the PLSR diagnostics. This mean model is the final model we report and use in application. The final step of the analysis involved application of the 1000 models to the 20% of the data that were originally split from the full data set (and never used) to report model performance on independent data (referred to as "independent validation" in our results).

Finally, we performed a series of post-hoc analyses on our spectroscopic predictions across our 13 field sites, 46 species, 165 plots, and 1226 samples to ensure that patterns of relationships among the spectroscopically determined traits match ecologically expected trends.

RESULTS

Leaf properties

Laboratory analyses showed large variation in the seven measured leaf traits across the 46 species and 13 study sites (Table 2). For M_{area} and N_{mass}, the distribution of values was significantly different (t test, $P < 0.05$) between the broadleaf and needleleaf tree species, while the remaining leaf traits displayed a similar range in values between the two leaf physiognomic groups. On a mass basis, nitrogen concentration (N_{mass}; %) varied more than sixfold across samples in the calibration data set, while leaf carbon (C_{mass}; %) exhibited the smallest trait variation (20.5%) among samples, but the C:N ratio showed a much larger distribution in values (10.5 to 68.6, data not shown), given the marked variation in N_{mass} (Table 2). M_{area} ranged from 17 to 270 g/m^2 across samples and species, falling somewhere in the middle of the global range (Table 2). Foliar recalcitrance properties (ADF, ADL, cellulose) were, on average, 9.4%, 6.2%, and 2.2% higher, respectively, for needleleaf vs. broadleaf tree leaves, while $\delta^{15}N$ displayed comparable variation between groups.

Leaf PLSR analyses

The reflectance of the dried and ground leaf material varied by 20–50% across the spectrum, and was comparable for both needleleaf and broadleaf samples

/TITAN/Production/e/ecap/live_jobs/ecap-24-07/ecap-24-07-08/layouts/ecap-24-07-08.3d ■ Monday, 22 September 2014 ■ 1:42 pm ■ Allen Press, Inc. ■ Page 1657 MS 13-2110

TABLE 4. Continued.

Trait vegetation type	N	Spectra	Spectral region (m)	Spectral treatment	R^2 Cal.	R^2 Val.
Temperate/boreal	372	dry	400–2498	2D[log(1/R)]	0.87	0.87, 0.74, 0.72
Montane conifer	132	dry	400–1098	2D[log(1/R)]	0.82	0.42
Montane conifer	132	dry	1100–2498	2D[Log(1/R)]	0.81	0.39
Mediterranean	182	dry	1100–2500	log(1/R)	0.95	0.93
Mediterranean	182	dry	1100–2500	1D[log(1/R)]	0.96	0.95
Mediterranean	182	dry	1100–2500	2D[log(1/R)]	0.97	0.89
Humid tropical	6136	fresh	400–1050	raw	0.32	
Humid tropical	6136	fresh	400–2500	raw	0.62	
Cellulose (%)						
Temperate/boreal	205	dry	1200–2400	log(1/R)	0.77	0.72
Temperate/boreal	372	dry	400–2498	1D[log(1/R)]	0.89	0.86, 0.87, 0.69
Temperate/boreal	372	dry	400–2498	2D[log(1/R)]	0.89	0.86, 0.84, 0.69
Temperate/boreal	372	dry	400–2498	2D[log(1/R)]	0.89	0.86, 0.83, 0.64
Montane conifer	132	dry	400–1098	2D[Log(1/R)]	0.88	0.70
Montane conifer	132	dry	1100–2498	2D[log(1/R)]	0.97	0.94
Mediterranean	182	dry	1100–2500	log(1/R)	0.97	0.97
Mediterranean	182	dry	1100–2500	1D[log(1/R)]	0.98	0.97
Mediterranean	182	dry	1100–2500	2D[log(1/R)]	0.98	0.96
Humid tropical	6136	fresh	400–1050	raw	0.27	
Humid tropical	6136	fresh	400–2500	raw	0.77	
δ^{15}N (‰)						
Temperate/boreal	178	dry	1200–2400	log(1/R)	0.62	0.60
Open savanna		fresh	619,695	raw	0.82	
Open savanna		fresh	603,704	1D[log(1/R)]	0.92	
Bog species	72	dry	1250–2350	log(1/R)	0.97	0.95
Bog species	72	dry	1250–2350	1D[log(1/R)]	0.98	0.91
Bog species	72	dry	1250–2350	2D[log(1/R)]	0.99	0.96
Managed pasture	37	dry	2036–2180	NBDA	0.34	

Notes: The number of samples shown represents the total number of observations used in the model calibration and validation (when available). Except for δ^{15}N, which had a limited number of studies, we did not include any previous studies utilizing multiple linear regression (MLR) models, given the issues reported by Grossman et al. (1996). Cells showing three values for the validation R^2 and the validation error measurement are drawn from studies using multiple data sets. Cells left blank indicate no data. NBDA stands for normalized band-depth analysis (Kokaly and Clark 1999). D refers to the level of derivative (i.e. difference) spectra used; 1D is first-difference, and 2D is the second-difference spectra.

† Error measurement was RMSE.

‡ Error measurement was the standard error of cross validation (SECV).

§ Error measurement was the standard error of prediction (SEP).

¶ Only reporting statistics for foliage samples.

Only reporting statistics for models developed using needles sampled from trees does not include falling needles or litter samples.

|| Study utilized stepwise multiple linear regressions to develop calibration model.

(Fig. 2), although the variance of the broadleaf samples was larger in the SWIR (Fig. 2b), while the variability in the NIR region was higher for needleleaf species (Fig. 2c).

All seven leaf traits included in this study were predicted with high accuracy and precision using the PLSR approach on reflectance measurements of dried and ground leaf material (Table 3, Fig. 3). The PLSR model for leaf nitrogen concentration (N_{mass}) exhibited the highest overall model calibration and validation performance (Fig. 3a, calibration $R^2 = 0.98$, calibration RMSE = 0.10%), followed by M_{area} (Fig. 3b, calibration $R^2 = 0.91$, calibration RMSE = 17.2 g/m^2) and leaf fiber concentration (Fig. 3c, calibration $R^2 = 0.84$, calibration RMSE = 2.8%). The models for C_{mass} (Fig. 3d), cellulose (Fig. 3e), and ADL (Fig. 3f) displayed moderate PLSR model performance with the percentage of RMSE between 7.2% and 12.7%, while δ^{15}N (Fig. 3g) showed the lowest overall predictive accuracy (Table 3). For the C_{mass} model, the small range in values (Table 2, Fig. 3d) likely contributed to the lower performance of the model; despite the lower R^2, note the reasonable RSME (11.1% of the trait range for validation data). Overall, our results are in line with those reported previously (Table 4).

We used the variable importance in projection (VIP) metric to identify the regions of the spectrum that were significant to the individual model calibrations (Fig. 4). Overall, the VIP values displayed consistent patterns across the spectrum, with notable variations correspond-

/TITAN/Production/e/ecap/live_jobs/ecap-24-07/ecap-24-07-08/layouts/ecap-24-07-08.3d ■ Monday, 22 September 2014 ■ 1:43 pm ■ Allen Press, Inc. ■ Page 1658 MS 13-2110

TABLE 4. Continued. Extended.

Error measurement		
Cal.	Val.	Source
1.64‡	1.65, 1.82, 5.29§	Bolster et al. (1996)¶
1.08‡	2.0†	Richardson and Reeves (2005)
1.12‡	1.64†	Richardson and Reeves (2005)
1.25‡	0.93§	Petisco et al. (2006)
1.19‡	0.85§	Petisco et al. (2006)
1.45‡	1.11§	Petisco et al. (2006)
8.16†		Asner et al. (2011*a*)
6.18†		Asner et al. (2011*a*)
1.4†	1.9†	this study
2.10‡	2.34, 1.76, 3.94§	Bolster et al. (1996)¶
2.14‡	2.35, 1.98, 3.08§	Bolster et al. (1996)¶
2.15‡	2.34, 2.04, 3.21§	Bolster et al. (1996)¶
1.30‡	2.69§	Richardson and Reeves (2005)
0.62‡	1.10§	Richardson and Reeves (2005)
1.10‡	0.88§	Petisco et al. (2006)
0.93‡	0.86§	Petisco et al. (2006)
1.10‡	0.98§	Petisco et al. (2006)
6.32†		Asner et al. (2011*a*)
2.47†		Asner et al. (2011*a*)
0.91†	1.51†	this study
(none reported)		Wang et al. (2007)‖
(none reported)		Wang et al. (2007)‖
1.89‡	1.60§	Kleinebecker et al. (2009)
1.84‡	1.99§	Kleinebecker et al. (2009)
1.70‡	1.42§	Kleinebecker et al. (2009)
1.78†		Elmore and Craine (2011)

ing to the contribution of particular wavelengths for leaf traits. For example, wavelengths in the SWIR region from 1900 to 2400 nm were uniformly important for all variables, but also varied in the position of peak importance among variables (Fig. 4). Close agreement between known spectral absorption features and significant wavelengths was observed for the seven leaf traits, especially the 1450 nm, 1690 nm, 1900 nm, 2100 nm, 2200 nm, and 2300 nm absorption features. The raw coefficients that can be applied to spectral reflectance plus their uncertainties are reported in Supplement 1 for all constituents.

The 1000× permutation analysis illustrates the uncertainty inherent in our seven PLSR models and in predictions made for each trait (Fig. 5, error bars). With the randomly selected training and test data (from the full calibration data set), we found that the spectral data continued to adequately predict leaf traits, but, as expected, with slightly lower accuracy and higher uncertainty (Fig. 5). The $\delta^{15}N$ model displayed the largest variability in results among the 1000 permutations and the N_{mass} model showed the smallest change in model performance. Some of the differences among models are related to variability in sample size and data range (Table 2), but a comparison of the standardized errors (%RMSE, Fig. 5b) indicates that, in general, the model error was similar among traits, excluding the very robust N_{mass} model. For $\delta^{15}N$, these results suggest that our models adequately capture the trend in isotopic ratio, but with lower relative precision than the other traits.

Ecological variation in leaf traits

We examined the ecological trends in spectroscopically predicted traits across our data set. N_{mass}, M_{area}, ADL, and $\delta^{15}N$ for the 15 most common broadleaf and needleleaf trees exhibited high variability within and among species across our sites (Fig. 6). In many cases,

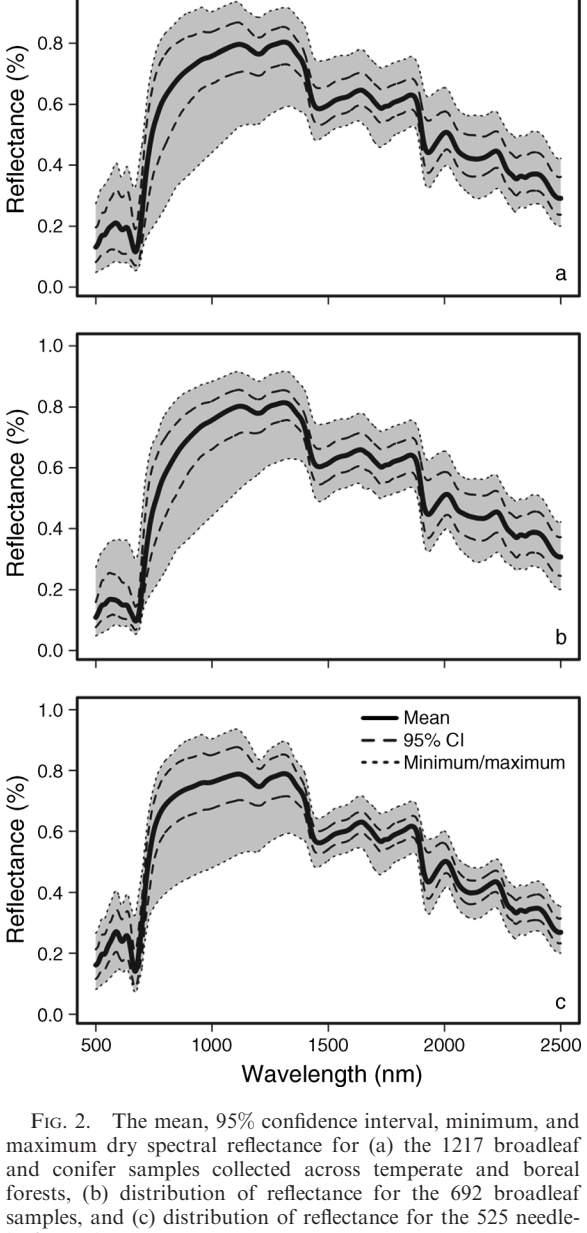

FIG. 2. The mean, 95% confidence interval, minimum, and maximum dry spectral reflectance for (a) the 1217 broadleaf and conifer samples collected across temperate and boreal forests, (b) distribution of reflectance for the 692 broadleaf samples, and (c) distribution of reflectance for the 525 needleleaf samples.

/TITAN/Production/e/ecap/live_jobs/ecap-24-07/ecap-24-07-08/layouts/ecap-24-07-08.3d ■ Monday, 22 September 2014 ■ 1:43 pm ■ Allen Press, Inc. ■ Page 1659 MS 13-2110

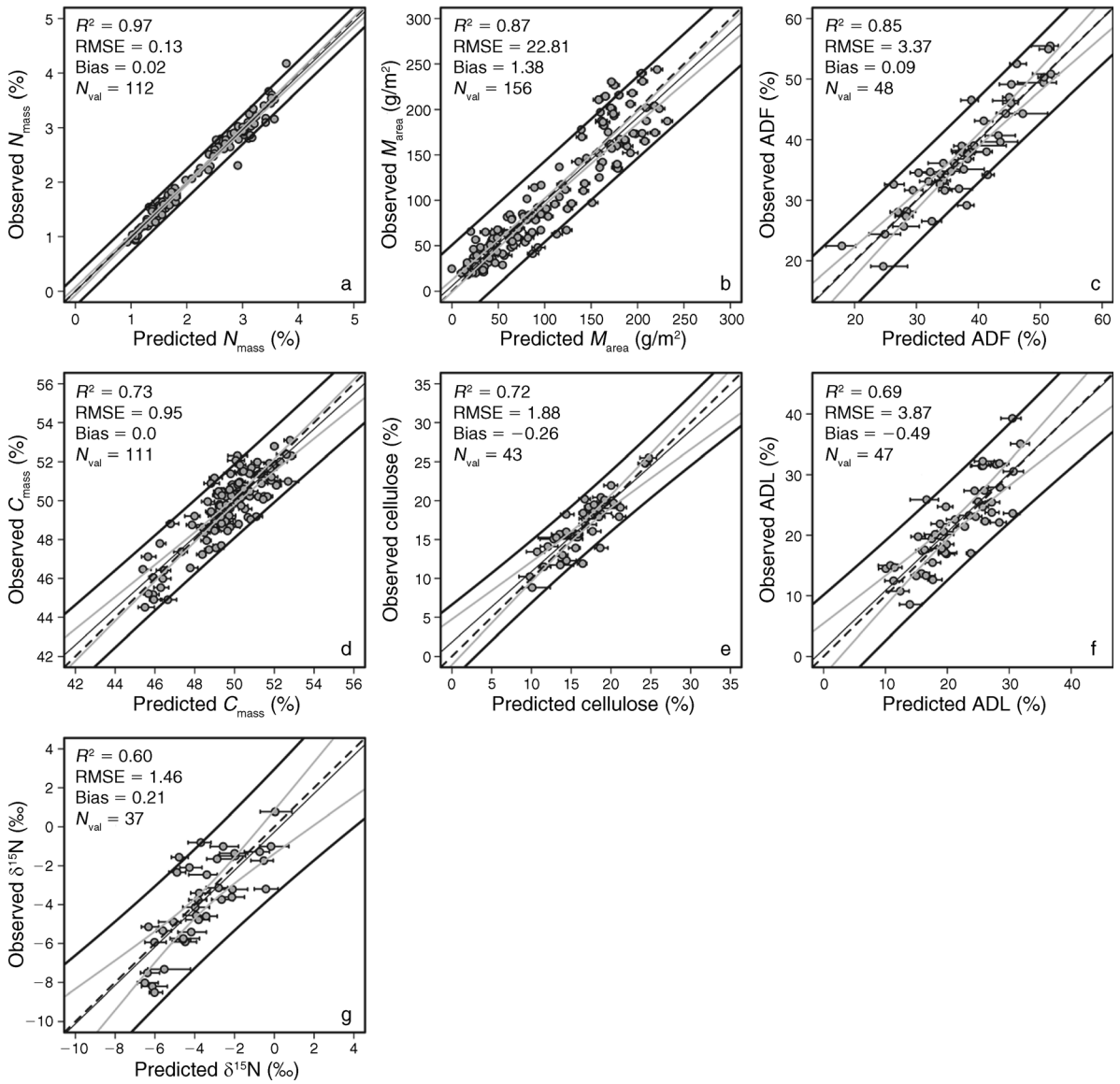

FIG. 3. Independent validation results for the seven partial least-squares regression (PLSR) models; nitrogen content (N_{mass}), carbon content (C_{mass}), isotopic composition ($\delta^{15}N$), leaf mass per area (M_{area}), acid-digestible fiber content (ADF), and acid-digestible lignin content (ADL). Error bars denote the 95% confidence intervals for each predicted value, while the dark lines denote the 95% prediction intervals and gray lines show the 95% confidence interval of the models. The dashed lines show the 1:1 line, with the regression line shown in light gray. Other abbreviations and variables are RMSE, root mean square error, and N_{val}. N_{val} refers to the number of independent observations used for validation of each PLSR model.

the within-species variation was as high as the variation across species, likely related to differences among layers in the canopy and ecological variations in site conditions. For M_{area}, canopy position (i.e., growing season light levels) played a strong role in mediating the values from the bottom to the top of the canopy, while N_{mass} did not display a significant change in values with canopy position (Fig. 7). However, nitrogen content (N_{area}, g/m^2; the product of M_{area} and N_{mass}) increased from the lower- to uppermost branches in the canopy, related to the strong changes in M_{area}, but the increase was greater for broadleaf trees (Fig. 7). For $\delta^{15}N$, we observed strong variation across sites related to broad climatic patterns, which in turn influence species composition and nutrient cycling (Fig. 8).

DISCUSSION

Our results for northern temperate and boreal forest tree species demonstrate the ability of dry-material spectra to characterize a wide range of foliar traits between and among species and functional types, as well as across the broad ecological gradients that drive between- and within-species variation in those traits. Moreover, we show that we can employ a single

/TITAN/Production/e/ecap/live_jobs/ecap-24-07/ecap-24-07-08/layouts/ecap-24-07-08.3d ■ Monday, 22 September 2014 ■ 1:43 pm ■ Allen Press, Inc. ■ Page 1660 MS 13-2110

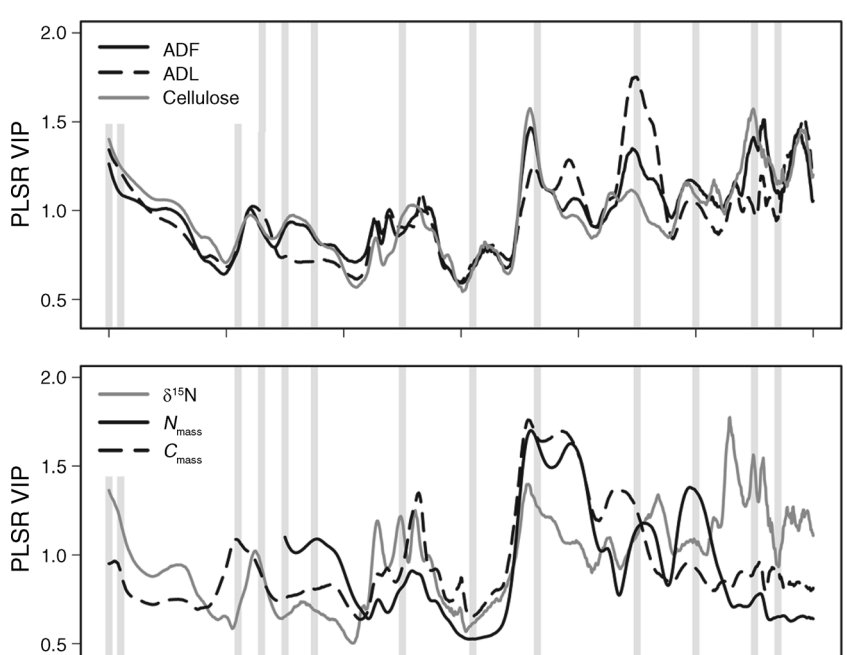

FIG. 4. The PLSR model variable importance of prediction (VIP) plot by wavelength for the six chemical constituents investigated in this study. The wavelength centers of key leaf chemical absorption features for leaf proteins, starches, cellulose, and lignin (Curran 1989, Elvidge 1990, Fourty et al. 1996) are presented as the vertical gray lines for reference.

calibration model per trait for all species and differing canopy positions among those species, suggesting a rapid and cost-effective approach to the quantification of geographic variation in foliar traits. Our results are comparable to previous studies using PLSR approaches (e.g., Bolster et al. 1996, Gillon et al. 1999, Brinkmann et al. 2002, Richardson and Reeves 2005, Petisco et al. 2006, Asner et al. 2011*a*; Table 4) and other methods (e.g., McLellan et al. 1991*a*, Martin and Aber 1994, Kokaly and Clark 1999, Curran et al. 2001). We observed the best model performance for the N_{mass} model, which is consistent with previous research (e.g., Bolster et al. 1996, Petisco et al. 2006); however our model for M_{area} was also strong (Table 3, Fig. 3b), with accuracy similar to results derived from fresh-leaf spectroscopy (e.g., Ourcival et al. 1999, Asner et al. 2011*a*; Table 4). The PLSR models for other leaf traits displayed slightly lower performance (Table 3, Figs. 3 and 5), but are within the range of results expected from the literature, several of which used fresh-leaf spectra observations (Table 4).

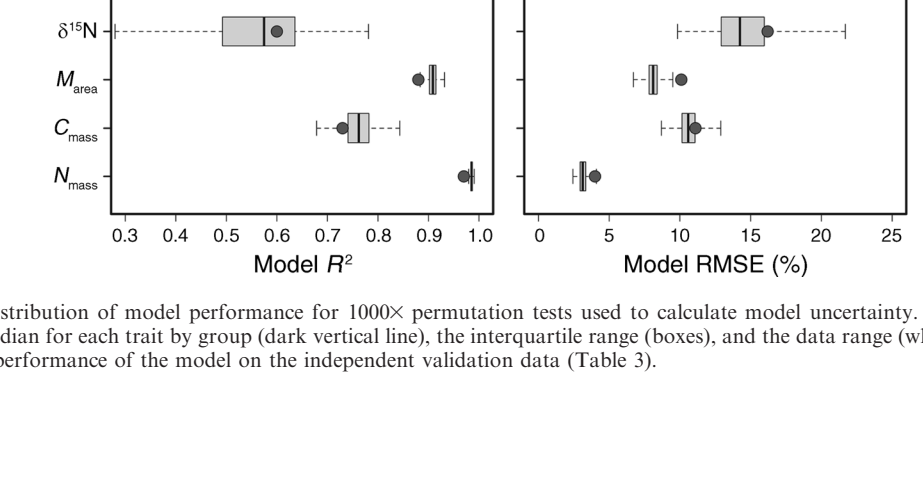

FIG. 5. Distribution of model performance for 1000× permutation tests used to calculate model uncertainty. The boxplots display the median for each trait by group (dark vertical line), the interquartile range (boxes), and the data range (whiskers). Gray dots indicate performance of the model on the independent validation data (Table 3).

/TITAN/Production/e/ecap/live_jobs/ecap-24-07/ecap-24-07-08/layouts/ecap-24-07-08.3d ■ Monday, 22 September 2014 ■ 1:43 pm ■ Allen Press, Inc. ■ Page 1661 MS 13-2110

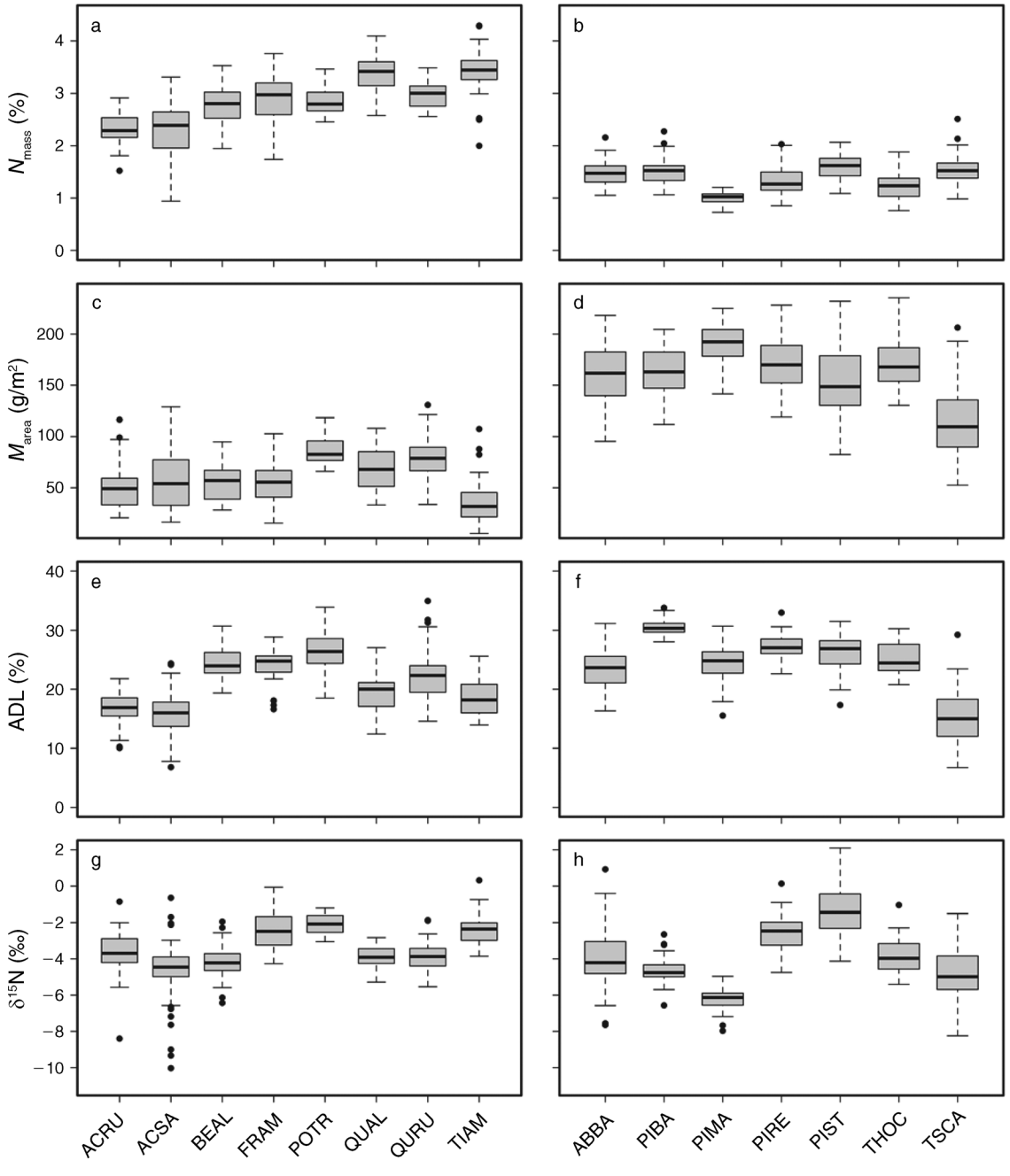

FIG. 6. Trait variability determined from spectroscopy for eight common broadleaf (left column) and seven common needleleaf (right column) species. Traits measured are (a, b) nitrogen concentration, (c, d) leaf mass per area, (e, f) lignin concentration, and (g, h) isotopic ^{15}N ratio. Species measured are red maple (ACRU), sugar maple (ACSA), yellow birch (BEAL), white ash (FRAM), trembling aspen (POTR), white oak (QUAL), northern red oak (QURU), American basswood (TIAM), balsam fir (ABBA), jack pine (PIBA), black spruce (PIMA), red pine (PIRE), white pine (PIST), northern white cedar (THOC), and eastern hemlock (TSCA). Boxplots display the median for each trait by group (dark horizontal line), the interquartile range (boxes), the data range (whiskers), and the extreme observations (black dots).

However, in contrast to many previous studies (Table 4), we avoided the use of first or higher order difference spectra. Permutations using derivative as opposed to raw spectra showed that such transformations yield unstable models because of the additional noise in the derivative spectra and the resulting influence this noise has on the PLSR regression coefficients (data not shown). Although several of the leaf traits we tested have been examined elsewhere, our study is unique in that we examined a large number of species (46) and traits (seven) concurrently, and analyzed leaves from different canopy levels (top third, middle third, and bottom third), following a

/TITAN/Production/e/ecap/live_jobs/ecap-24-07/ecap-24-07-08/layouts/ecap-24-07-08.3d ■ Monday, 22 September 2014 ■ 1:43 pm ■ Allen Press, Inc. ■ Page 1662 MS 13-2110

consistent analytical approach. Furthermore, we included a comprehensive uncertainty analysis within our PLSR modeling step. The coefficients reported in Supplement 1 can be applied to spectra recorded in a fashion consistent with our methods to estimate these traits for temperate and boreal taxa similar to those in our data set.

Our results reinforce the utility of spectroscopic methods for quantitatively estimating a range of key foliar properties, including M_{area} (LMA), N_{mass}, and structural components (e.g., lignin, cellulose), across diverse tree species (Figs. 3 and 4). Unlike the use of narrow-band spectral vegetation indices (SVIs) for the estimation of key leaf traits (e.g., Gitelson et al. 2006, Le Maire et al. 2008), our PLSR approach characterizes the simultaneous contribution of many important absorption properties of leaves (e.g., Curran 1989, Fourty et al. 1996, Foley et al. 1998; Fig. 4) to the overall relationship with leaf reflectance, generally yielding more robust models when compared to SVIs (Feret et al. 2011). Specifically, the locations of important wavelengths in our biochemical PLSR models match the locations of known spectral absorption features related to proteins, nitrogen, lignin, cellulose, and starches (Curran 1989, Elvidge 1990, Fourty et al. 1996, Kokaly et al. 2009; Fig. 4). However, differences in important wavelengths among traits (Fig. 4) and in the associated prediction coefficients (Supplement 1) demonstrate that the relationships between spectral features and foliar traits vary considerably, emphasizing that different components of the spectrum are sensitive to different chemical constituents or leaf traits.

The ability to accurately estimate leaf chemistry using reflectance spectroscopy depends on instrument characteristics (e.g., spectral resolution, signal-to-noise, which has steadily improved in recent years), the magnitude of the optical signal for the trait of interest, and the availability of foliage samples spanning a sufficient range of values (Curran 1989, Foley et al. 1998, Feret et al. 2011). In addition, the measurement precision of the analytical techniques to develop calibration data can vary among the traits of interest. In particular, the methods for determining ADF and lignin ADL concentration can result in relatively high variance between replicate samples (Brinkmann et al. 2002). This is due to the gravimetric methods used to determine the values for ADF and ADL; cellulose is determined as the difference between the two. In our data set, we estimate from sample replicates that measurement error for ADF and ADL is between 1% and 12%, but generally less than 5%. Similarly, we found considerable replicate variance for the $\delta^{15}N$ samples, ranging from 1% to 10%. Likewise, the methods used for estimating needleleaf M_{area} are also known to introduce error (Bond-Lamberty et al. 2003), primarily due to the difficulty in accurately measuring the projected area of needles. A review of the literature suggests that a model for M_{area} may be improved by the use of fresh-leaf spectroscopic data (Table 4), given the strong coupling between water content, leaf structure, and M_{area} (Fourty and Baret 1997, Asner et al. 2011*a*, *b*).

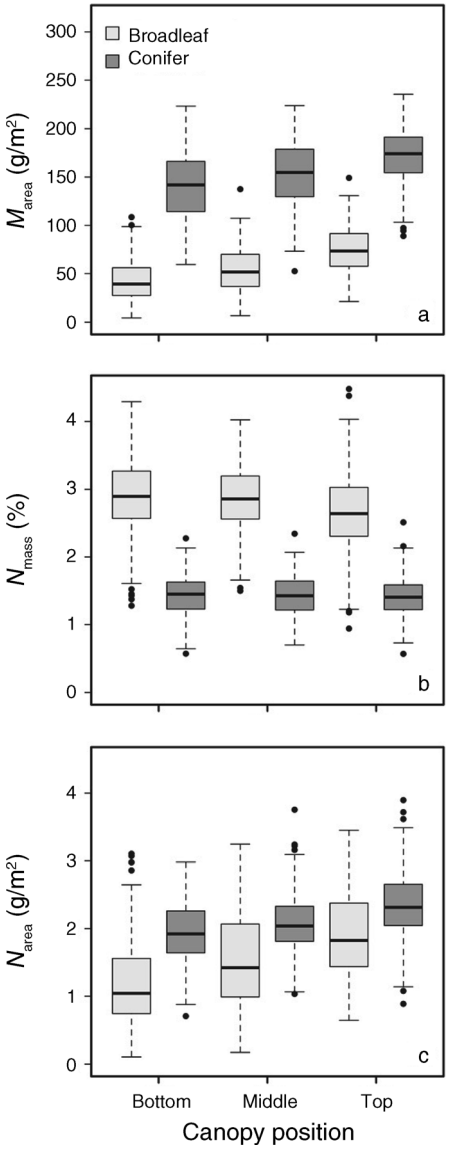

FIG. 7. Trait variation by canopy position (bottom one-third, middle one-third, top one-third of canopy) determined from spectroscopy for (a) leaf mass per area, (b) nitrogen concentration, and (c) nitrogen content. Boxplots display the median for each trait by group (dark horizontal line), the interquartile range (boxes), the data range (whiskers), and the extreme observations (black dots).

Our study differs significantly from previous research in that we did not limit our collection of foliar samples to the top, sunlit portion of the crown (e.g., Asner et al. 2011*a*), nor did we aggregate samples from differing needle ages in evergreen conifer species (e.g., Petisco et al. 2006). The resulting PLSR models were able to successfully integrate all the variation related to species, canopy position, and physiognomic differentiation (Table 2, Appendix A) into a single model

/TITAN/Production/e/ecap/live_jobs/ecap-24-07/ecap-24-07-08/layouts/ecap-24-07-08.3d ■ Monday, 22 September 2014 ■ 1:43 pm ■ Allen Press, Inc. ■ Page 1663 MS 13-2110

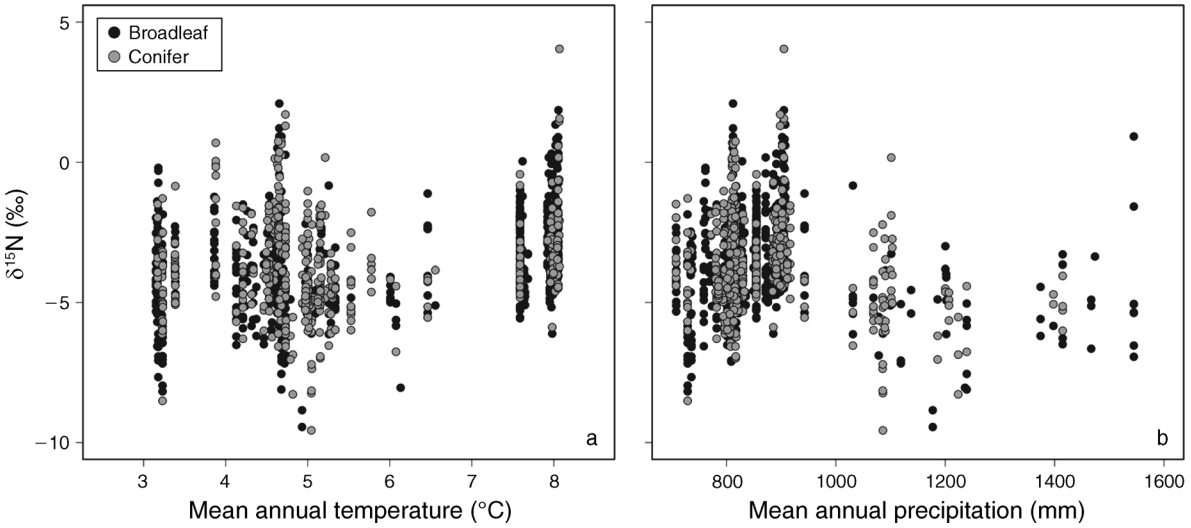

FIG. 8. Patterns across broad climatic gradients of foliar isotopic concentration ($\delta^{15}N$) determined from spectroscopy. (a) Relationship of foliar $\delta^{15}N$ with mean annual temperature. (b) Relationship of foliar $\delta^{15}N$ with mean annual precipitation. The black filled circles show the patterns of broadleaf tree species, while the gray filled circles display the patterns of needle-leaf tree species. Climate data were derived from PRISM (Daly et al. 1994). Patterns closely match those derived from a global data set (Craine et al. 2009).

for each trait (Table 3, Fig. 3). The results did not show sensitivity of the models to species type, canopy position, or leaf lifespan (Appendix B). This demonstrates that we can use these models to rapidly assess important within-canopy variations in leaf traits that are ecologically significant to whole-plant nutrient dynamics, light harvesting, and carbon sequestration. The within-canopy variation is often ignored when estimating canopy or stand level variables for ecosystem process models, some of which can utilize this information directly (e.g., Drewry et al. 2010), and other analyses due to the logistics of sample collection or analytical expense. The key finding is that spectra reflect the variations in leaf properties within a canopy, thereby enabling spectroscopy retrieval of traits without having to stratify the analyses by canopy position.

Spectroscopic determination of foliar isotopes

Several previous studies explored the potential to estimate foliar isotopic concentrations of leaf nitrogen ($\delta^{15}N$) and carbon ($\delta^{13}C$), reporting accuracy levels of 70–99% (Richardson and Reeves 2005, Wang et al. 2007, Kleinebecker et al. 2009). However, Elmore and Craine (2011) did not observe a strong relationship between spectral reflectance of dried and ground leaf material and $\delta^{15}N$ ($R^2 = 0.34$). In addition, they did not observe a strong relationship between leaf nitrogen and $\delta^{15}N$, which they hypothesized as one of the more likely reasons for which previous studies observed an ability to estimate $\delta^{15}N$ from leaf reflectance spectroscopy. We observed only a moderate correlation between $\delta^{15}N$ and leaf nitrogen percentage (N_{mass}, $r = 0.32$), suggesting covariance with N_{mass} may have only provided a minor contribution to our ability to predict $\delta^{15}N$. However, given the prediction $R^2 = 0.62$ for $\delta^{15}N$ from spectra, it is unlikely that the weak correlation between $\delta^{15}N$ and N_{mass} alone explains our ability to estimate $\delta^{15}N$, and that spectroscopic sensitivity to $\delta^{15}N$ is a real feature rather than an artifact of a $\delta^{15}N$–N_{mass} correlation. Much work is still required to develop full confidence in the ability to estimate $\delta^{15}N$ from spectroscopy: our model for $\delta^{15}N$ was not as strong as that reported by Kleinebecker et al. (2009), which may result from sample size ($N = 72$ compared to our $N = 178$) or scope of species included. Nevertheless, the results of our study and others (Richardson and Reeves 2005, Kleinebecker et al. 2009) highlight the potential for the spectroscopic determination of foliar isotopes, even if only broadly, and represent an important prospect for ecological studies.

Broad applications of contact spectroscopy for ecological studies

Use of rapid spectroscopic methods to characterize foliar traits imparts considerable savings in both time and analytical expense, allowing for a larger number of measurements to be made across broader geographic regions. This increase in measurement capacity leads to a greater ability to both characterize within- and between-species variability and to test hypotheses about spatial variability in foliar traits with respect to climatic and other drivers (e.g., disturbance legacies; Deel et al. 2012). For instance, ecosystem models often assume constant values of traits per species, when in fact these traits can vary considerably within a species (Fig. 6).

/TITAN/Production/e/ecap/live_jobs/ecap-24-07/ecap-24-07-08/layouts/ecap-24-07-08.3d ■ Monday, 22 September 2014 ■ 1:43 pm ■ Allen Press, Inc. ■ Page 1664 MS 13-2110

However, we can now utilize information on trait variability to better simulate variation and uncertainty in ecosystem responses to climate, global change, and disturbances (LeBauer et al. 2013). Moreover, traits vary within canopies, in particular in response to the light environment (Niinemets 2007). Most notably, M_{area} is higher in the sunlit portion of a canopy, and declines with lower canopy position (Fig. 7). Although nitrogen concentration by mass (N_{mass}) does not vary considerably within a canopy (Fig. 7), nitrogen content by area (N_{area}), a key determinant of photosynthetic capacity (Kattge et al. 2009), is highly variable as a consequence of the variability in M_{area} within canopies (Fig. 7). In terms of characterizing the recalcitrance properties of foliage (e.g., ADL, cellulose, $\delta^{15}N$), our spectroscopic methods yielded estimates that match expected ecological patterns across species types (Fig. 6e–h), describing the potential turnover rates and nitrogen cycling potential (Melillo et al. 1982) across a much larger sample than is logistically feasible with standard approaches. For example, isotopic analysis can be prohibitive but, despite our reported limitations, patterns of $\delta^{15}N$ derived from spectra with respect to climate follow the results of Craine et al. (2009) quite well. The ability to utilize rapid and inexpensive spectroscopic methods to quantify the patterns of foliar traits allows for meaningful data to be feasibly generated across a wide variety of species, canopy heights, and study locations. Also, further refinement of laboratory spectroscopic techniques provides increased support for refining algorithms useful for predicting these traits from canopy-level imaging spectrometer data (e.g., AVIRIS; Green et al. 1998).

Generalized algorithms of leaf functional traits

Building on our results, future work should concentrate on linking similar data and observations from around the world (e.g., Bolster et al. 1996, Asner et al. 2011*a*, Doughty et al. 2011) to develop globally generalized models (e.g., Martin et al. 2008, Feret et al. 2011). Numerous studies have illustrated the potential for remotely sensing foliar biochemistry at a variety of scales and with fresh or dry leaf spectra (e.g., Wessman et al. 1988*a*, *b*, Bolster et al. 1996, Martin and Aber 1997, Richardson and Reeves 2005, Petisco et al. 2006, Asner et al. 2011*a*), yet a general set of models covering the larger suite of leaf traits worldwide does not exist. For intensive projects such as the U.S. National Ecological Observatory Network (NEON; Kampe et al. 2010) and the Carnegie Spectranomics project (Asner and Martin 2009), which have large remote sensing and leaf-based spectroscopy components, it is becoming increasingly important to standardize methods and provide operational algorithms that can be applied both at the leaf level and from remote sensing platforms.

Future spaceborne imaging spectrometers such as the proposed Hyperspectral Infrared Imager (HyspIRI) will allow for the repeat, global mapping of key ecosystem parameters, such as N_{mass} and M_{area}. Further work will help identify the extent to which leaf-level spectral features scale to the pixel. Our study and others, such as Feret et al. (2011) and Asner et al. (2011*a*), provide a foundation for such efforts and should help to distinguish the candidate traits for generalized multiscale models (e.g., N_{mass}, M_{area}, lignin) from those that may not scale efficiently (e.g., $\delta^{15}N$). In particular, the development of standardized approaches to retrieve foliar traits from leaf-level spectra across many species provides the basis to identify and compare spectral features in canopy-level spectra that are related to these same traits. The correspondence of spectral features to foliar traits in multiple types of spectral data (dry, fresh, canopy spectra) points to a convergence of foliar optical properties that we can leverage to more fully characterize the variability in ecological function of ecosystems across broad geographical areas (Townsend et al. 2013). Future work will address spectral variability in fresh spectra and imaging spectroscopy using these same species, sample locations, and study sites.

Conclusions

The characterization of foliar chemistry composition and morphology is essential to understanding the response of forest ecosystems to continued global change. In this study, we found that a number of important leaf structural and biochemical traits could be accurately estimated utilizing spectroscopic data, collected on dried and ground leaf material, and a partial least-squares regression (PLSR) approach. These included leaf nitrogen concentration (N_{mass}; %), carbon concentration (C_{mass}; %), leaf mass per area (M_{area}; g/m^2), fiber (ADF; %), lignin (ADL; %), cellulose (%), and the nitrogen isotopic composition ($\delta^{15}N$; ‰). In particular, N_{mass} was strongly related to leaf spectra ($R^2 = 0.98$), as were fiber constituents (R^2 of 0.77–0.84) and leaf mass per area ($R^2 = 0.91$). The wavelength contributions were broadly similar for the seven leaf traits, but also displayed significant distinctions in specific wavelengths of importance, especially within the shortwave infrared (SWIR) region. In addition, the wavelengths of highest importance corresponded to spectral regions of known chemical absorption features, including those related to foliar proteins, lignin, cellulose, and starches. An important next step for this type of remote sensing research is to combine similar data sets for other ecosystems (e.g., Richardson and Reeves 2005, Petisco et al. 2006, Asner et al. 2011*a*) to refine and standardize both data and methods as a basis for operational models to estimate foliar traits from vegetation globally. Such information will facilitate more rapid and geographically broader characterization of the range of variability in vegetation traits (and our uncertainty in estimating them) for ecological research, remote sensing, and modeling.

/TITAN/Production/e/ecap/live_jobs/ecap-24-07/ecap-24-07-08/layouts/ecap-24-07-08.3d ■ Monday, 22 September 2014 ■ 1:43 pm ■ Allen Press, Inc. ■ Page 1665 MS 13-2110

Acknowledgments

Funding for this research was provided by NASA Terrestrial Ecology grant NNX08AN31G to P. A. Townsend and B. E. McNeil and a NASA Earth and Space Science Fellowship grant NNX08AV07H to S. P. Serbin. Thank you to J. Limbach, B. Isaacson, A. Edgerton, L. Deel, B. Breslow, C. Parana, and C. Leibfried for field and laboratory assistance, and to E. Kruger, S. T. Gower and C. Kucharik for helpful comments on earlier versions of this paper. Finally, we would like to thank two anonymous reviewers for the helpful comments that greatly improved an earlier version of the manuscript.

Literature Cited

Aber, J. D., and J. M. Melillo. 1982. Nitrogen immobilization in decaying hardwood leaf litter as a function of initial nitrogen and lignin content. Canadian Journal of Botany 60:2261–2269.

Abràmoff, M. D., P. J. Magalhaes, and S. J. Ram. 2004. Image processing with ImageJ. Biophotonics International 11:36–42.

Ahl, D. E., S. T. Gower, D. S. Mackay, S. N. Burrows, J. M. Norman, and G. R. Diak. 2004. Heterogeneity of light use efficiency in a northern Wisconsin forest: implications for modeling net primary production with remote sensing. Remote Sensing of Environment 93:168–178.

Asner, G. P., and R. E. Martin. 2008. Spectral and chemical analysis of tropical forests: scaling from leaf to canopy levels. Remote Sensing of Environment 112:3958–3970.

Asner, G. P., and R. E. Martin. 2009. Airborne spectranomics: mapping canopy chemical and taxonomic diversity in tropical forests. Frontiers in Ecology and the Environment 7:269–276.

Asner, G. P., R. E. Martin, D. E. Knapp, R. Tupayachi, C. Anderson, L. Carranza, P. Martinez, M. Houcheime, F. Sinca, and P. Weiss. 2011*a*. Spectroscopy of canopy chemicals in humid tropical forests. Remote Sensing of Environment 115:3587–3598.

Asner, G. P., R. E. Martin, R. Tupayachi, R. Emerson, P. Martinez, F. Sinca, G. V. N. Powell, S. J. Wright, and A. E. Lugo. 2011*b*. Taxonomy and remote sensing of leaf mass per area (LMA) in humid tropical forests. Ecological Applications 21:85–98.

Baret, F., and T. Fourty. 1997. Estimation of leaf water content and specific leaf weight from reflectance and transmittance measurements. Agronomie 17:455–464.

Bolster, K. L., M. E. Martin, and J. D. Aber. 1996. Determination of carbon fraction and nitrogen concentration in tree foliage by near infrared reflectance: a comparison of statistical methods. Canadian Journal of Forest Research 26:590–600.

Bond-Lamberty, B., C. Wang, and S. T. Gower. 2003. The use of multiple measurement techniques to refine estimates of conifer needle geometry. Canadian Journal of Forest Research 33:101–105.

Bowling, D. R., D. E. Pataki, and J. T. Randerson. 2008. Carbon isotopes in terrestrial ecosystem pools and CO_2 fluxes. New Phytologist 178:24–40.

Brinkmann, K., L. Blaschke, and A. Polle. 2002. Comparison of different methods for lignin determination as a basis for calibration of near-infrared reflectance spectroscopy and implications of lignoproteins. Journal of Chemical Ecology 28:2483–2501.

Burrows, S. N., S. T. Gower, J. M. Norman, G. Diak, D. S. Mackay, D. E. Ahl, and M. K. Clayton. 2003. Spatial variability of aboveground net primary production for a forested landscape in northern Wisconsin. Canadian Journal of Forest Research 33:2007–2018.

Burton, J. I., D. J. Mladenoff, M. K. Clayton, and J. A. Forrester. 2011. The roles of environmental filtering and colonization in the fine-scale spatial patterning of ground-layer plant communities in north temperate deciduous forests. Journal of Ecology 99:764–776.

Card, D. H., D. L. Peterson, P. A. Matson, and J. D. Aber. 1988. Prediction of leaf chemistry by the use of visible and near infrared reflectance spectroscopy. Remote Sensing of Environment 26:123–147.

Chen, S., X. Hong, C. J. Harris, and P. M. Sharkey. 2004. Spare modeling using orthogonal forest regression with PRESS statistic and regularization. IEEE Transaction on Systems, Man and Cybernetics 34:898–911.

Compton, J. E., T. D. Hooker, and S. S. Perakis. 2007. Ecosystem N distribution and $\delta^{15}N$ during a century of forest regrowth after agricultural abandonment. Ecosystems 10:1197–1208.

Cook, B. D., P. V. Bolstad, J. G. Martin, F. A. Heinsch, K. J. Davis, W. G. Wang, A. R. Desai, and R. M. Teclaw. 2008. Using light-use and production efficiency models to predict photosynthesis and net carbon exchange during forest canopy disturbance. Ecosystems 11:26–44.

Cornwell, W. K., et al. 2008. Plant species traits are the predominant control on litter decomposition rates within biomes worldwide. Ecology Letters 11:1065–1071.

Couture, J., T. Meehan, and R. Lindroth. 2011. Atmospheric change alters foliar quality of host trees and performance of two outbreak insect species. Oecologia 1–14.

Craine, J. M., et al. 2009. Global patterns of foliar nitrogen isotopes and their relationships with climate, mycorrhizal fungi, foliar nutrient concentrations, and nitrogen availability. New Phytologist 183:980–992.

Curran, P. J. 1989. Remote-sensing of foliar chemistry. Remote Sensing of Environment 30:271–278.

Curran, P. J., J. L. Dungan, and D. L. Peterson. 2001. Estimating the foliar biochemical concentration of leaves with reflectance spectrometry: testing the Kokaly and Clark methodologies. Remote Sensing of Environment 76:349–359.

Curran, P. J., J. A. Kupiec, and G. M. Smith. 1997. Remote sensing the biochemical composition of a slash pine canopy. IEEE Transactions on Geoscience and Remote Sensing 35:415–420.

Curtis, J. T. 1959. The vegetation of Wisconsin: an ordination of plant communities. Second edition. University of Wisconsin Press, Madison, Wisconsin, USA.

Dahlin, K. M., G. P. Asner, and C. B. Field. 2013. Environmental and community controls on plant canopy chemistry in a Mediterranean-type ecosystem. Proceedings of the National Academy of Sciences USA 110:6895–6900.

Daly, C., R. P. Neilson, and D. L. Phillips. 1994. A statistical topographic model for mapping climatological precipitation over mountainous terrain. Journal of Applied Meteorology 33:140–158.

Dawson, T. P., P. J. Curran, and S. E. Plummer. 1998. LIBERTY—modeling the effects of leaf biochemical concentration on reflectance spectra. Remote Sensing of Environment 65:50–60.

Deel, L. N., B. E. McNeil, P. G. Curtis, S. P. Serbin, A. Singh, K. N. Eshleman, and P. A. Townsend. 2012. Relationship of a Landsat cumulative disturbance index to canopy nitrogen and forest structure. Remote Sensing of Environment 118:40–49.

Desai, A. R., et al. 2008. Influence of vegetation and seasonal forcing on carbon dioxide fluxes across the Upper Midwest, USA: implications for regional scaling. Agricultural and Forest Meteorology 148:288–308.

Doughty, C., G. Asner, and R. Martin. 2011. Predicting tropical plant physiology from leaf and canopy spectroscopy. Oecologia 165:289–299.

Drewry, D. T., P. Kumar, S. Long, C. Bernacchi, X. Z. Liang, and M. Sivapalan. 2010. Ecohydrological responses of dense canopies to environmental variability: 1. Interplay between vertical structure and photosynthetic pathway. Journal of Geophysical Research—Biogeosciences 115.

/TITAN/Production/e/ecap/live_jobs/ecap-24-07/ecap-24-07-08/layouts/ecap-24-07-08.3d ■ Monday, 22 September 2014 ■ 1:43 pm ■ Allen Press, Inc. ■ Page 1666 MS 13-2110

Ecarnot, M., F. Compan, and P. Roumet. 2013. Assessing leaf nitrogen content and leaf mass per unit area of wheat in the field throughout plant cycle with a portable spectrometer. Field Crops Research 140:44–50.

Elmore, A. J., and J. M. Craine. 2011. Spectroscopic analysis of canopy nitrogen and nitrogen isotopes in managed pastures and hay land. IEEE Transactions on Geoscience and Remote Sensing 49:2491–2498.

Elvidge, C. D. 1990. Visible and near-infrared reflectance characteristics of dry plant materials. International Journal of Remote Sensing 11:1775–1795.

Evans, J. R. 1989. Photosynthesis and nitrogen relationships in leaves of C_3 plants. Oecologia 78:9–19.

Ewers, B. E., D. S. Mackay, J. Tang, P. V. Bolstad, and S. Samanta. 2008. Intercomparison of sugar maple (*Acer saccharum* Marsh.) stand transpiration responses to environmental conditions from the western Great Lakes region of the United States. Agricultural and Forest Meteorology 148:231–246.

Fassnacht, K. S., and S. T. Gower. 1999. Comparison of the litterfall and forest floor organic matter and nitrogen dynamics of upland forest ecosystems in north central Wisconsin. Biogeochemistry 45:265–284.

Feilhauer, H., G. P. Asner, R. E. Martin, and S. Schmidtlein. 2010. Brightness-normalized partial least squares regression for hyperspectral data. Journal of Quantitative Spectroscopy and Radiative Transfer 111:1947–1957.

Feret, J. B., C. Francois, G. P. Asner, A. A. Gitelson, R. E. Martin, L. P. R. Bidel, S. L. Ustin, G. le Maire, and S. Jacquemoud. 2008. PROSPECT-4 and 5: advances in the leaf optical properties model separating photosynthetic pigments. Remote Sensing of Environment 112:3030–3043.

Feret, J. B., C. Francois, A. Gitelson, G. P. Asner, K. M. Barry, C. Panigada, A. D. Richardson, and S. Jacquemoud. 2011. Optimizing spectral indices and chemometric analysis of leaf chemical properties using radiative transfer modeling. Remote Sensing of Environment 115:2742–2750.

Field, C., and H. A. Mooney. 1986. The photosynthesis-nitrogen relationship in wild plants. Pages 22–55 *in* T. Givnish, editor. On the economy of plant form and function. Cambridge University Press, Cambridge, UK.

Foley, S., B. Rivard, G. A. Sanchez-Azofeifa, and J. Calvo. 2006. Foliar spectral properties following leaf clipping and implications for handling techniques. Remote Sensing of Environment 103:265–275.

Foley, W. J., A. Mcllwee, I. Lawler, L. Aragones, A. P. Woolnough, and N. Berding. 1998. Ecological applications of near infrared reflectance spectroscopy—a tool for rapid, cost-effective prediction of the composition of plant and animal tissues and aspects of animal performance. Oecologia 116:293–305.

Fortunel, C., et al. 2009. Leaf traits capture the effects of land use changes and climate on litter decomposability of grasslands across Europe. Ecology 90:598–611.

Fourty, T., and F. Baret. 1997. Vegetation water and dry matter contents estimated from top-of-the-atmosphere reflectance data: a simulation study. Remote Sensing of Environment 61:34–45.

Fourty, T., F. Baret, S. Jacquemoud, G. Schmuck, and J. Verdebout. 1996. Leaf optical properties with explicit description of its biochemical composition: direct and inverse problems. Remote Sensing of Environment 56:104–117.

Frelich, L. E., and C. G. Lorimer. 1991. Natural disturbance regimes in hemlock hardwood forests of the Upper Great Lakes region. Ecological Monographs 61:145–164.

Frelich, L. E., and P. B. Reich. 1995. Neighborhood effects, disturbance, and succession in forests of the western Great Lakes Region. Ecoscience 2920:148–158.

Ganapol, B. D., L. F. Johnson, P. D. Hammer, C. A. Hlavka, and D. L. Peterson. 1998. LEAFMOD: a new within-leaf radiative transfer model. Remote Sensing of Environment 63:182–193.

Geladi, P., and B. R. Kowalski. 1986. Partial least-squares regression—a tutorial. Analytica Chimica Acta 185:1–17.

Gillon, D., C. Houssard, and R. Joffre. 1999. Using near-infrared reflectance spectroscopy to predict carbon, nitrogen and phosphorus content in heterogeneous plant material. Oecologia 118:173–182.

Gitelson, A. A., G. P. Keydan, and M. N. Merzlyak. 2006. Three-band model for noninvasive estimation of chlorophyll, carotenoids, and anthocyanin contents in higher plant leaves. Geophysical Research Letters 33: 5.

Green, D. S., J. E. Erickson, and E. L. Kruger. 2003. Foliar morphology and canopy nitrogen as predictors of light-use efficiency in terrestrial vegetation. Agricultural and Forest Meteorology 115:165–173.

Green, R. O., et al. 1998. Imaging spectroscopy and the airborne visible infrared imaging spectrometer (AVIRIS). Remote Sensing of Environment 65:227–248.

Grossman, Y. L., S. L. Ustin, S. Jacquemoud, E. W. Sanderson, G. Schmuck, and J. Verdebout. 1996. Critique of stepwise multiple linear regression for the extraction of leaf biochemistry information from leaf reflectance data. Remote Sensing of Environment 56:182–193.

Helliker, B. R., and S. L. Richter. 2008. Subtropical to boreal convergence of tree-leaf temperatures. Nature 454:511–514.

Hobbie, J. E., and E. A. Hobbie. 2006. ^{15}N in symbiotic fungi and plants estimates nitrogen and carbon flux rates in Arctic tundra. Ecology 87:816–822.

Jacquemoud, S., and F. Baret. 1990. PROSPECT—a model of leaf optical properties of spectra. Remote Sensing of Environment 34:75–91.

Kampe, T. U., B. R. Johnson, M. Kuester, and M. Keller. 2010. NEON: the first continental-scale ecological observatory with airborne remote sensing of vegetation canopy biochemistry and structure. Journal of Applied Remote Sensing 4(043510).

Kattge, J., W. Knorr, T. Raddatz, and C. Wirth. 2009. Quantifying photosynthetic capacity and its relationship to leaf nitrogen content for global-scale terrestrial biosphere models. Global Change Biology 15:976–991.

Kleinebecker, T., S. R. Schmidt, C. Fritz, A. J. P. Smolders, and N. Holzel. 2009. Prediction of $\delta^{13}C$ and $\delta^{15}N$ in plant tissues with near-infrared reflectance spectroscopy. New Phytologist 184:732–739.

Kokaly, R. F., G. P. Asner, S. V. Ollinger, M. E. Martin, and C. A. Wessman. 2009. Characterizing canopy biochemistry from imaging spectroscopy and its application to ecosystem studies. Remote Sensing of Environment 113:S78–S91.

Kokaly, R. F., and R. N. Clark. 1999. Spectroscopic determination of leaf biochemistry using band-depth analysis of absorption features and stepwise multiple linear regression. Remote Sensing of Environment 67: 267–287.

le Maire, G., C. François, K. Soudani, D. Berveiller, J. Y. Pontailler, N. Bréda, H. Genet, H. Davi, and E. Dufrêne. 2008. Calibration and validation of hyperspectral indices for the estimation of broadleaved forest leaf chlorophyll content, leaf mass per area, leaf area index and leaf canopy biomass. Remote Sensing of Environment 112:3846–3864.

LeBauer, D. S., and K. K. Treseder. 2008. Nitrogen limitation of net primary productivity in terrestrial ecosystems is globally distributed. Ecology 89:371–379.

LeBauer, D. S., D. Wang, K. T. Richter, C. C. Davidson, and M. C. Dietze. 2013. Facilitating feedbacks between field measurements and ecosystem models. Ecological Monographs 83:133–154.

Martin, M. E., and J. D. Aber. 1994. Analyses of forest foliage III: determining nitrogen, lignin, and cellulose in fresh leaves using near infrared reflectance data. Journal of Near Infrared Spectroscopy 2:25–32.

/TITAN/Production/e/ecap/live_jobs/ecap-24-07/ecap-24-07-08/layouts/ecap-24-07-08.3d ■ Monday, 22 September 2014 ■ 1:43 pm ■ Allen Press, Inc. ■ Page 1667 MS 13-2110

Martin, M. E., and J. D. Aber. 1997. High spectral resolution remote sensing of forest canopy lignin, nitrogen, and ecosystem processes. Ecological Applications 7:431–443.

Martin, M. E., L. C. Plourde, S. V. Ollinger, M. L. Smith, and B. E. McNeil. 2008. A generalizable method for remote sensing of canopy nitrogen across a wide range of forest ecosystems. Remote Sensing of Environment 112:3511–3519.

Matson, P., L. Johnson, C. Billow, J. Miller, and R. L. Pu. 1994. Seasonal patterns and remote spectral estimation of canopy chemistry across the Oregon transect. Ecological Applications 4:280–298.

McLellan, T. M., J. D. Aber, M. E. Martin, J. M. Melillo, and K. J. Nadelhoffer. 1991*a*. Determination of nitrogen, lignin, and cellulose content of decomposition leaf material by near-infrared reflectance spectroscopy. Canadian Journal of Forest Research 21:1684–1688.

McLellan, T. M., M. E. Martin, J. D. Aber, J. M. Melillo, K. J. Nadelhoffer, and B. Dewey. 1991*b*. Comparison of wet chemistry and near-infrared reflectance measurements of carbon-fraction chemistry and nitrogen concentration of forest foliage. Canadian Journal of Forest Research 21:1689–1693.

McNeil, B. E., J. M. Read, T. J. Sullivan, T. C. McDonnell, I. J. Fernandez, and C. T. Driscoll. 2008. The spatial pattern of nitrogen cycling in the Adirondack Park, New York. Ecological Applications 18:438–452.

Melillo, J. M., J. D. Aber, and J. F. Muratore. 1982. Nitrogen and lignin control of hardwood leaf litter decomposition dynamics. Ecology 63:621–626.

Mevik, B. H., and R. Wehrens. 2007. The pls package: principal component and partial least squares regression in R. Journal of Statistical Software 18:1–24.

Mitchell, M. J., D. J. Raynal, and C. T. Driscoll. 1996. Biogeochemistry of a forested watershed in the central Adirondack Mountains: temporal changes and mass balances. Water, Air and Soil Pollution 88:355–369.

Niinemets, U. 2007. Photosynthesis and resource distribution through plant canopies. Plant, Cell and Environment 30:1052–1071.

Ollinger, S. V. 2011. Sources of variability in canopy reflectance and the convergent properties of plants. New Phytologist 189:375–394.

Ollinger, S. V., and M. L. Smith. 2005. Net primary production and canopy nitrogen in a temperate forest landscape: an analysis using imaging spectroscopy, modeling and field data. Ecosystems 8:760–778.

Ollinger, S. V., M. L. Smith, M. E. Martin, R. A. Hallett, C. L. Goodale, and J. D. Aber. 2002. Regional variation in foliar chemistry and N cycling among forests of diverse history and composition. Ecology 83:339–355.

Ourcival, J. M., R. Joffre, and S. Rambal. 1999. Exploring the relationships between reflectance and anatomical and biochemical properties in *Quercus ilex* leaves. New Phytologist 143:351–364.

Pastor, J., J. D. Aber, C. A. McClaugherty, and J. M. Melillo. 1984. Aboveground production and N and P cycling along a nitrogen mineralization gradient on Blackhawk Island, Wisconsin. Ecology 65:256–268.

Peterson, D. L., J. D. Aber, P. A. Matson, D. H. Card, N. Swanberg, C. Wessman, and M. Spanner. 1988. Remote sensing of forest canopy and leaf biochemical contents. Remote Sensing of Environment 24:85–108.

Petisco, C., B. Garcia-Criado, S. Mediavilla, B. R. V. de Aldana, I. Zabalgogeazcoa, and A. Garcia-Ciudad. 2006. Near-infrared reflectance spectroscopy as a fast and non-destructive tool to predict foliar organic constituents of several woody species. Analytical and Bioanalytical Chemistry 386:1823–1833.

Poorter, H., U. Niinemets, L. Poorter, I. J. Wright, and R. Villar. 2009. Causes and consequences of variation in leaf mass per area (LMA): a meta-analysis. New Phytologist 182:565–588.

R Development Core Team. 2013. R: a language and environment for statistical computing. R Foundation for Statistical Computing, Vienna, Austria. www.r-project.org

Richardson, A. D., G. P. Berlyn, and T. G. Gregoire. 2001. Spectral reflectance of *Picea rubens* and *Abies balsamea* needles along an elevational gradient, Mt. Moosilauke, New Hampshire, USA. American Journal of Botany 88:667–676.

Richardson, A. D., and J. B. Reeves. 2005. Quantitative reflectance spectroscopy as an alternative to traditional wet lab analysis of foliar chemistry: near-infrared and mid-infrared calibrations compared. Canadian Journal of Forest Research 35:1122–1130.

Robinson, D. 2001. $\delta^{15}N$ as an integrator of the nitrogen cycle. Trends in Ecology and Evolution 16:153–162.

Santiago, L. S. 2007. Extending the leaf economics spectrum to decomposition: evidence from a tropical forest. Ecology 88:1126–1131.

Schulte, L. A., D. J. Mladenoff, S. N. Burrows, T. A. Sickley, and E. V. Nordheim. 2005. Spatial controls of pre-Euro-American wind and fire disturbance in northern Wisconsin (USA) forest landscapes. Ecosystems 8:73–94.

Serbin, S. P., D. N. Dillaway, E. L. Kruger, and P. A. Townsend. 2012. Leaf optical properties reflect variation in photosynthetic metabolism and its sensitivity to temperature. Journal of Experimental Botany 63:489–502.

Shipley, B., D. Vile, E. Garnier, I. J. Wright, and H. Poorter. 2005. Functional linkages between leaf traits and net photosynthetic rate: reconciling empirical and mechanistic models. Functional Ecology 19:602–615.

Smith, M. L., M. E. Martin, L. Plourde, and S. V. Ollinger. 2003. Analysis of hyperspectral data for estimation of temperate forest canopy nitrogen concentration: comparison between an airborne (AVIRIS) and a spaceborne (Hyperion) sensor. IEEE Transactions on Geoscience and Remote Sensing 41:1332–1337.

Smith, M. L., S. V. Ollinger, M. E. Martin, J. D. Aber, R. A. Hallett, and C. L. Goodale. 2002. Direct estimation of aboveground forest productivity through hyperspectral remote sensing of canopy nitrogen. Ecological Applications 12:1286–1302.

Townsend, P. A., J. R. Foster, R. A. Chastain, and W. S. Currie. 2003. Application of imaging spectroscopy to mapping canopy nitrogen in the forests of the central Appalachian Mountains using Hyperion and AVIRIS. IEEE Transactions on Geoscience and Remote Sensing 41:1347–1354.

Townsend, P. A., S. P. Serbin, E. L. Kruger, and J. A. Gamon. 2013. Disentangling the contribution of biological and physical properties of leaves and canopies in imaging spectroscopy data. Proceedings of the National Academy of Sciences USA 110:E1074.

Ustin, S. L., A. A. Gitelson, S. Jacquemoud, M. Schaepman, G. P. Asner, J. A. Gamon, and P. Zarco-Tejada. 2009. Retrieval of foliar information about plant pigment systems from high resolution spectroscopy. Remote Sensing of Environment 113:S67–S77.

Wang, L. X., G. S. Okin, J. Wang, H. Epstein, and S. A. Macko. 2007. Predicting leaf and canopy ^{15}N compositions from reflectance spectra. Geophysical Research Letters 34(2):L02401.

Wessman, C. A., J. D. Aber, D. L. Peterson, and J. M. Melillo. 1988*a*. Foliar analysis using near-infrared reflectance spectroscopy. Canadian Journal of Forest Research 18:6–11.

Wessman, C. A., J. D. Aber, D. L. Peterson, and J. M. Melillo. 1988*b*. Remote-sensing of canopy chemistry and nitrogen cycling in temperate forest ecosystems. Nature 335:154–156.

White, M. K., S. T. Gower, and D. E. Ahl. 2005. Life cycle inventories of roundwood production in northern Wisconsin:

/TITAN/Production/e/ecap/live_jobs/ecap-24-07/ecap-24-07-08/layouts/ecap-24-07-08.3d ■ Monday, 22 September 2014 ■ 1:43 pm ■ Allen Press, Inc. ■ Page 1668 MS 13-2110

inputs into an industrial forest carbon budget. Forest Ecology and Management 219:13–28.

Wold, S. 1994. PLS for multivariate linear modeling. Pages 195–218 *in* H. van de Waterbeemd, editor. Chemometric methods in molecular design, methods and principles in medicinal chemistry. Verlag-Chemie, Weinheim, Germany.

Wold, S., A. Ruhe, H. Wold, and W. J. Dunn. 1984. The collinearity problem in linear regression. The partial least-squares (PLS) regression approach to generalized inverses. Siam Journal on Scientific and Statistical Computing 5(3):735–743.

Wold, S., M. Sjostrom, and L. Eriksson. 2001. PLS-regression: a basic tool of chemometrics. Chemometrics and Intelligent Laboratory Systems 58:109–130.

Wolter, P. T., P. A. Townsend, B. R. Sturtevant, and C. C. Kingdon. 2008. Remote sensing of the distribution and abundance of host species for spruce budworm in northern Minnesota and Ontario. Remote Sensing of Environment 112:3971–3982.

Wright, I. J., et al. 2004. The worldwide leaf economics spectrum. Nature 428:821–827.

Supplemental Material

Appendix A

List of tree species and their estimated functional trait values (*Ecological Archives* A024-198-A1).

Appendix B

Analysis of the partial least-squares regression (PLSR) model residuals (*Ecological Archives* A024-198-A2).

Supplement 1

The resulting PLSR model coefficients (and their uncertainties) for predicting foliar traits using leaf-level dried and ground spectral reflectance data (*Ecological Archives* A024-198-A3).

Supplement 2

Simplified R script file illustrating the calibration of the dry spectra PLSR models and associated uncertainty analysis (*Ecological Archives* A024-198-A4).

/TITAN/Production/e/ecap/live_jobs/ecap-24-07/ecap-24-07-08/layouts/ecap-24-07-08.3d ■ Monday, 22 September 2014 ■ 1:43 pm ■ Allen Press, Inc. ■ Page 1669 MS 13-2110